A Critical Review of the Measurement of Ice Adhesion to Solid Substrates

Andrew Work[1], Yongsheng Lian[2]

([1] Ohio Aerospace Institute, corresponding author, email address: andrew.h.work@nasa.gov)

([2] University of Louisville)

Pre-print, published edition available here: https://doi.org/10.1016/j.paerosci.2018.03.001

1 Contents

2 ABSTRACT

Ice adhesion is an issue spanning a wide range of technical fields. In the aerospace industry, ice accretion has led to a large number of casualties and costs the industry billions of dollars every year. To design effective anti-/de-icing systems, the adhesion of ice to surfaces must be understood. In this review paper, the authors surveyed for papers providing methods for the measurement of ice adhesion. 113 papers were identified for comparison, with data being extracted from 58 papers with common test surfaces (aluminum, steel, Teflon® (Chemours), and polyurethane). The methods used were categorized and data were compared based on their precision and the trends they demonstrated. Conceptual problems were identified with the tests used in the literature and discussed, and open questions relevant to testing the adhesion of ice were identified. Several key parameters affecting ice adhesion identified from the literature were temperature, surface roughness, strain rate, and impact velocity. Their effects on adhesion strength were discussed. While researching this topic, it was discovered that many papers did not report the strain rate in their tests, and the vast majority of papers did not correct their data for stress concentrations on the surface, either of which has been shown to cause variation in the data by one order of magnitude. Data compared from the literature typically spanned one to three orders of magnitude. The causes of these variations were discussed.

3 Nomenclature

3D	three-dimensional
AERTS	Adverse Environment Rotor Test Stand
AMIL	Anti-icing Materials International Laboratory
ARF	Adhesion Reduction Factor
CAT	Centrifuge Adhesion Test
CCAT	calculated Centrifuge Adhesion Test
CF	centripetal force
FEA	finite element analysis
ICAT	instrumented Centrifuge Adhesion Test
IRT	Icing Research Tunnel
LVDT	linear variable differential transformer
LWC	liquid water content
MVD	mean volume diameter
NACA	National Advisory Committee for Aeronautics
PSU	Penn State University

PVDF polyvinylidene fluoride

SP sample preserving

1 Introduction

The buildup of ice on aircraft is a deadly multibillion-dollar-per-year problem in the aerospace industry [1, 2]. While there are many crucial aspects to the problem, ice adhesion to aircraft structures is the driving cause of the problem. Early papers documenting attempts to combat ice adhesion date back at least as far as 1930 where qualitative comparisons were made in an open-plenum icing tunnel at the National Advisory Committee for Aeronautics (NACA) Langley [3, 4]. The earliest test methods to measure the adhesion of ice occurred prior to 1940 [5]. These early papers investigated several concepts, including the application of surface coatings, now termed "icephobics." These early coatings included greases, oils, soluble compounds, paints, and more. While there has been considerable effort to measure the adhesion of ice to more common substrates since these early works (both with impact ice relevant to aircraft icing and other types of ice), the literature only tends to agree on a broad range of adhesion strengths spanning one to three orders of magnitude. Unfortunately, most of the data available is for ice created at conditions unrealistic to in-flight conditions.

Because of the long history of adhesion testing on ice, there is a significant body of work on the subject. Unfortunately, much of this work is rarely cited and quite difficult to find; this has built up into a significant problem in the literature. Older papers generally discussed the adhesion on a more fundamental level, with open discussion of the problems in testing adhesion. At the time, the technology did not exist to answer these questions and much of the necessary capability has only become available in the last decade. Authors stopped discussing these problems in their papers, and it has since become standard practice to ignore many important aspects of testing ice adhesion. Despite this, many current researchers are aware of these problems.

A significant potential pitfall for those wishing to obtain data for the design of aircraft components is that some authors broadly cite applications for their work to include aircraft, but do not run their adhesion tests using impact ice. A classic example of this is Teflon®, which has a large range of adhesion strength (typically low) when tests are run using nonimpact ice [6-9] and high adhesion strength when using impact ice [10, 11]. Combined with the fact that the earliest adhesion tests on low-ice-adhesion surfaces date back to at least the 1930s [3] with no successful commercial product developed to date, there is skepticism in the industry over the effectiveness of new products and no widely accepted method to test them.

Recently, many researchers have begun to publish papers on low-ice-adhesion surfaces (which may be included in the broadly used term icephobic) with experimental data [12-17]. The primary goal of these papers is not to develop a new method to measure the

adhesion of ice. As a result, the quality of the data in the literature represents a problem for authors developing new surfaces. Because the data covers such a large range, an author presenting a test method will have an easy time finding sources that obtained similar values, providing easy but poor validation for their test. This comparison is better between similar methods, but the most popular methods report a wide range of values. While there are a multitude of authors using a broad range of test methods, several methods are starting to emerge as favorites in the literature. The two most prominent are the Centrifuge Adhesion Test (CAT) [18] and the pusher test that uses a cuvette as a mold for the ice [19].

Several reviews exist in the literature on the development of new icephobic surfaces [20-22], but they do not provide suitable detail on the testing of these surfaces as they are focused on a broader category of information. There are several papers in the literature that specifically review the test methods used to measure the adhesion of ice, either as a review paper or in the introduction of a research paper [23-27]. The most recent review, by Schulz, is a very important paper demonstrating the problem of the state of stress at the interface in tests used for ice adhesion [25]. However, this paper is limited in scope, only showing the results of finite element analysis (FEA) modeling to demonstrate the mixed state of stress at the interface. The oldest review, by Oksanen, is also discussed in the Lap Shear Tests section [26]. Oksanen's paper is one of few papers that presents data on the effect of strain rate on ice and contains helpful discussion on the subject. Many of these papers have useful discussions and provide some of the only documentation available for some more obscure papers. The review by Kasaai et al. is perhaps the only dedicated review in the literature on the methods used to measure the adhesion of ice [23]. This 2004 review discusses tests in a qualitative manner. Unfortunately, the discussion has a narrow application since it only captures a small number of tests and misses many important aspects of these tests. The authors of this paper disagree with several of their conclusions, such as the possibility of using peel or cantilever tests, and many of their recommendations were not subsequently tested by researchers and therefore cannot be justified from the literature.

The purpose of the current review is to gather a large amount of data from the literature to compare the efficacy of current test methods and address problems encountered when testing ice through an extensive literature survey. Other topics are also of primary concern to the measurement of the adhesion of impact ice, such as the material properties of the ice (tensile strength or elastic modulus) and by extension the manner in which the ice was grown. Generally speaking, there is little material data available on impact ice; many authors cite Hobbs for polycrystalline ice [28], but some data specific to impact ice is available in the literature [29-31]. Furthermore, not all facilities are calibrated in the same manner, meaning that the ice grown under the same reported parameters at one facility may not have the same material properties as ice grown in another facility with the same reported parameters (for data on the calibration of the Icing Research Tunnel (IRT) at the NASA Glenn Research Center, see [32, 33]). This paper is focused on the measurement of

the adhesion of ice, and since these topics are not discussed further, the reader is advised to consult the literature.

Because of the large number of variables involved, direct comparisons must be given cautiously. It is impossible to make a perfect comparison while matching all the important variables across papers in the literature because many of these important variables were not reported. Many authors do not record detailed roughness features or wetting characteristics and generalizations are often made on the substrate that they used. They usually do not match ice formation conditions, the strain rate is often unrecorded and almost never varied, stress concentrations are almost universally ignored and highly variable, and surface preparation methods are often different. As such, data in this paper are generally grouped irrespective of certain variables, such as the roughness of the substrate, to allow for comparison. All data used in this paper are provided in a Microsoft Excel spreadsheet with the supplemental data. Several papers sought for inclusion in this review were unavailable; these are cited for the reader's convenience [34-44].

This paper presents the methods for measuring the adhesion of ice found in the literature in categorized sections. Each section contains a list of references for papers fitting that category and a discussion summarizing the important features of the tests in each category. After each discussion section, there is a section that presents data from papers in that category and a discussion on that data. Following the discussion of individual categories of tests is a discussion of the literature as a whole, then a section comparing data from all categories of tests, and finally the conclusions section.

1.1 Data Gathering Methods

Data were extracted from several papers and tabulated for comparison. Much of the data were only available in the form of plots and converted using WebPlotDigitizer [45]. Values were double-checked visually. Some of the plots are of poor quality (generally in the older papers), where the axes were not orthogonal to each other, and the vertical axes were angled. In these cases, images of the plots were rotated to align the axes as well as possible. Data points extracted from a plot are marked as such in the supplemental material.

The terminology used herein is as follows. A "data point" includes an average and standard deviation calculated from a set of repeat tests. This set of repeat results includes the original test result plus any duplicates run at the same condition and using the same test method, sourced from the same paper. A "repeat" is any one of the test results reported at the same condition in a set of repeats (e.g., no repeats were performed if only one test result is recorded, but two repeats were performed if two test results (an original and a duplicate) were recorded at the same conditions). All data points include a minimum of two repeats. A data set includes multiple data points. Data may refer to recorded test conditions at a particular data point, or the values of the data points obtained for this paper.

All variables were converted into SI units, generally using kPa for the adhesion strength. The adhesion strength, test temperature, and impact velocity were considered

primary variables. Any other variables were considered secondary variables; these were recorded into the data set for this paper based on the authors' interpretation of what was intended in the original paper to be a repeated data point. The average of the repeats was used when values varied by small amounts in a qualitative manner. For example, in plot-extracted data, the authors may have used cylinders of different sizes, and multiple data points recorded with a 2 cm diameter cylinder may be extracted from the plot with diameters of 1.9, 2.0, and 2.1 cm. In this case, the average of 2.0 cm would be recorded. For secondary data presented as a range in the papers, if a maximum and minimum value were provided, the average was recorded; if only a maximum or a minimum value was given, it was recorded unmodified. The data were then reduced, averaging the adhesion strength values of duplicate test points. The standard deviation of the duplicate points was calculated and recorded. Several papers presented duplicate data from prior publications. When this was suspected to be the case, the duplicate data were omitted from extraction from all papers but the earliest one found. Examples include data shown in References [46, 47, 48, 49]. For the purpose of collecting data, alloys of aluminum and steel were grouped together with aluminum and steel data, respectively. Unless otherwise noted, average standard deviations are taken by directly averaging the percent standard deviation of each averaged data point irrespective of the number of repeats at any point.

2 Ice Adhesion Measurement Methods

The methods used to measure ice adhesion can be sorted a variety of ways, but here they are sorted into three categories: centrifuge tests, common direct mechanical tests (direct mechanical tests simply being tests where the mechanical force is applied directly), and miscellaneous tests. Centrifuge tests represent the narrowest group, but represent a large section of the current literature [12, 18, 34, 46, 47, 50-71]. Common direct mechanical tests include push tests [10, 11, 16, 17, 19, 48, 49, 72-104] and shear tests (such as a lap joint shear test) [6-9, 13, 105-122]. These tests are fundamentally different from centrifuge tests in that they do not require motion of the ice to generate force on the interface (indirectly providing the force, making centrifuge tests indirect mechanical tests), can be run on a universal test machine, and preserve the test sample (in a centrifuge test, the ice is destroyed on separation). Miscellaneous tests include a wide variety of tests and citations are shown in their respective sections.

2.1 Centrifuge

While the use of a centrifuge to test the adhesion of ice predates Loughborough's work in 1946 [50], the archetype for the bulk of modern tests is the design used by the Anti-icing Materials International Laboratory (AMIL), introduced in 2005 [18]. Loughborough's system used a rotating plate coated with a sample and then used a mold to freeze an ice "button" to the sample. AMIL's design uses a rotating beam with a counterweight to reduce vibration due to an imbalance, and samples are fastened to the beam before each test (see Fig. 1). Sample preparation in AMIL's test can be done in batch off the centrifuge, under a spray stand, or even in a wind tunnel. Producing samples in batch is advantageous to test

the repeatability of the test method and for the efficiency of the test. This is supported by the fact that AMIL has produced at least 432 data points in the five years after the test was introduced [70], more than any other group has ever produced to date. In the same paper, AMIL introduced an update to their CAT method, the CAT-NG method, which improved the quality of data obtained. CAT is used to differentiate tests using AMIL's design from generic centrifuge adhesion tests grouped into other sections.

2.1.1 Centrifuge Adhesion Test

All centrifuge tests use centripetal forces to shear the ice from a test surface. AMIL's test uses a simple procedure in which the weighed sample of ice is spun at a constantly increasing rate until it separates. Separation is detected when the ice hits the centrifuge wall by piezoelectric cells, though other means could be used. The publications from AMIL, like most other papers, present the shear strength of ice to the substrate as $\tau = F / A$, which assumes a uniform stress distribution at the interface. Stress concentrations are present in AMIL's tests, and thus not directly accounted for. For a centrifuge sample with simplified geometry, Schulz shows the state of stress at the interface is complex, and that shear stresses predominantly act at the edges of the sample, while peel stresses dominate elsewhere [25].

To account for this nonuniform stress distribution, AMIL expresses their results in a comparative manner, using the Adhesion Reduction Factor (ARF). The ARF is equivalent to the adhesion strength of a baseline material as measured by the CAT divided by the adhesion strength of ice to the substrate of interest. By growing repeatable ice shapes and using statistically significant sample sizes, the stress concentration at the interface is expected to cancel out. Without detailed FEA using accurate sample geometries, this method cannot give quantitative, standalone results for the adhesion strength of ice, but it can provide an accurate comparison to a baseline material.

The baseline material of choice for AMIL, and in general for the CAT, is aluminum. Aluminum may be problematic because of oxidation of the interface, but otherwise provides a consistent substrate material. AMIL runs the bulk of their tests at –10 °C and makes samples in batch using consistent methods, providing relatively consistent geometry. The edges of ice formed from spray have random features that likely promote scatter in their results. The bulk of tests performed with the CAT use ice formed at low-impact speeds relevant to power line icing, but too slow for aircraft icing. Since ice is not tested in situ, samples must be grown remotely and brought to the test site, introducing a thermal and mechanical history to each sample. Residual stresses frozen into the interface may be allowed dissipate because of creep effects, and handling may introduce cracks at the interface, which is a concern primarily for low-ice-adhesion surfaces. Pre-cracking the interface should only reduce the adhesion, providing erroneously low data. The effect of residual stresses is poorly understood for impact ice since the formation process is complex and varies between different types of impact ice (e.g., rime versus glaze). For ice formed by pouring water into a mold (refrigerated ice), frozen stresses have a strong impact on the

adhesion strength of ice, which is shown by testing refrigerated ice frozen at different rates [73, 114].

Koivuluoto et al. included FEA in their analysis using simplified geometry [67]. They ran tests using ice at low-impact speeds not intended to be relevant for aircraft icing using an approach similar to AMIL's and through their FEA showed strong stress concentrations at the interface, particularly at the edge of the ice (see Fig. 2). Using simplified geometry will likely be problematic for aircraft ice because of the likelihood of strong variations in the geometry near the edges, requiring three-dimensional (3D) scans to accurately simulate the stresses at the edges. The authors noted that their superhydrophobic surfaces and hydrophobic surfaces with low roughness performed well as anti-icing materials, though it must be stressed that this was at low-impact speeds.

The CAT method has many other disadvantages. First, CAT samples are not preserved, making inspection of the sheared interface impossible. Second, stress-strain curves are not captured, precluding a more detailed analysis of results, and the relationship between the strain rate and adhesion strength is difficult to investigate. Third, CATs have variable ice geometry near the edges of the samples, likely creating variable stress concentrations, though they have good repeatability and this variation is likely small. If the variation is significant, it must be accounted for by testing large numbers of samples, possibly by 3D scanning the ice and running FEA on the scanned geometry or by some other means. The sharp edges of the samples are also not ideal for testing aircraft ice since the collection efficiency will vary sharply from the center of the sample to the edges, providing a variation in the type of ice collected in a single sample at higher speeds. Last, vibration and aerodynamic loading may also be present in CATs.

2.1.2 Calculated Centrifuge Adhesion Test

A similar method to test the adhesion strength of ice is the calculated CAT (CCAT). This method, used by Itagaki [51], involves calculating the adhesion strength and tensile strength of the ice based on the length of a shed piece of ice from a rotor. This addresses several of the issues of the CAT by testing the ice in situ (the ice is not moved or handled to test it) and reducing the edges used. In Itagaki's test, a cylinder was used to gather ice, which likely had issues related to vibration due to von Karman vortex shedding. This method also introduces new issues since the bulk properties of impact ice are poorly understood, and the ice gathered will vary over the length of the rotor since the impact speed will increase with increasing radial distance from the center of rotation. This method was also used by Fortin with an airfoil in a wind tunnel, notably at speeds reaching 130 m/s [62]. In 1991, Scavuzzo et al. also performed stress analysis of ice on rotors, though the computational power available at the time was a limiting factor [123].

2.1.3 Instrumented Centrifuge Adhesion Test

The final type of centrifuge test that was used by Penn State University (PSU), the Adverse Environment Rotor Test Stand (AERTS), is an instrumented CAT (ICAT). The

AERTS is a test stand on which a variety of rotors can be mounted. For adhesion testing, a 9-ft (2.74-m) rotor is mounted with an attachment at the end containing a custom-built force transducer and a coupon mount with an airfoil profile that stands ahead of the main rotor to prevent ice bridging. The AERTS stand and mount are shown in Fig. 3.

To grow ice, the facility has spray nozzles (of the same type used at Glenn's IRT) mounted in the ceiling. The nozzles create a cloud in the room that impacts the test surface with the rotor spinning. This way the impact velocity can be varied by varying the speed of the rotor. Cloud properties are controlled by adjusting the pressures to the nozzles. The force transducer in the AERTS allows the force to be measured while ice is accreting, and since the rotational velocity and radius is known, the mass can be measured. The rotors spin at a constant velocity and ice grows until a shed occurs. Once a shed occurs, the test is stopped and the interfacial area between the shed ice and the coupon is recorded using graph paper (see Fig. 4).

The use of ICAT for testing ice adhesion provides several advantages over other centrifuge tests. While a stress-strain curve cannot be provided, total interfacial stress is recorded as a function of time. The large diameter of the rotor allows larger sample sizes to be used while maintaining a very small variation in force across the sample because of centripetal loading. Another advantage is that the ice is tested in situ, requiring no handling. Perhaps the biggest advantage of this method is the ability to generate high-speed impact ice without a wind tunnel.

However, this method has a number of disadvantages. Like the other centrifuge methods, the presence of edges dictates that there will be varied collection efficiency near the ends of the coupon compared to the center of the model, and strain rates are difficult or impossible to predict. This latter effect is more pronounced for ICAT since the strain rate will vary with the growth of the ice, which is likely nonlinear as it depends on the ice geometry. More importantly, varying accretion conditions have a pronounced effect on the shape of the ice. As seen in Fig. 4(a) to (c), the ice geometry for a glaze condition is complex and overhangs the edges of the coupon on the same length scale as the coupon length. Other ice shapes produced in AERTS overhang less or not at all. This variation in geometry must produce significant variations in the stress concentration at the interface. The mount also has supports at the back and a variable radius of curvature that varies sample to sample. As shown in Fig. 4, the coupon sheet stands off of the mounting geometry. As the shape of the ice changes, the location of maximum stress will change. Even if this were not the case, this geometry is far more complex than that simulated by Schulz [25]. To correct the data, FEA needs to be run using detailed 3D scans of the ice to create the geometry file. Another problem is the applicability of results from ICAT methods to nonrotating aircraft surfaces. Rotating the geometry through accretion changes the runback path of the ice and may modify the crystal structure of the ice and the stresses frozen in the ice through accretion. It is also problematic because not all the ice shedding is due to an adhesive failure. A horn of ice that was not connected to the main piece of ice

shed and is shown in Fig. 4(a) and (d). These smaller separations occur near the main failure of the ice and will be difficult if not impossible to separate from the data. This will provide another source of scatter for ice shapes that are susceptible to shedding via cohesive breaks. Vibrational loading and aerodynamic loading are likely to be small, but they provide another source of loading on the ice to affect the shedding.

Centrifuge tests as a whole have reasonable scatter compared with other tests, but cannot provide a stress-strain curve and suffer from a variety of technical difficulties. Very little data is available from centrifuge tests comparing the adhesion at varying parameters, particularly at varying strain rates. This is particularly problematic for centrifuge tests since the strain rate has been shown to have a strong effect on the adhesion strength of ice [110]. Also by using typical test methods, the strain rate will vary depending on the mass of the ice (as in AMIL's tests) or the growth rate of the ice (as in PSU's tests) since the force on the ice is directly proportional to the mass of the ice. Despite the large amount of data, the influence of key variables on the adhesion strength of ice cannot be understood from the literature using centrifuge tests.

For centrifuge tests, the only methods to obtain in situ high-speed adhesion data are those used by Fortin [70] and the ICAT method. In the absence of a high-speed wind tunnel, these are the only methods to produce high-speed impact ice, which represents a significant cost savings. These methods are not recommended for providing quantitative adhesion data to use for the design of aircraft components, but provide a qualitative comparison between surfaces. Combining their use for qualitative comparison with the efficiency of obtaining data, they would serve well as screening tools to downselect surfaces to use for more expensive test methods. However, it is important to note that similar problems exist for all other test methods found by the authors in the literature, leaving no good alternatives to obtain quantitative data until new test methods emerge. Data obtained from centrifuge tests in the literature are shown in Fig. 5 and Fig. 6.

2.1.4 Centrifuge Data

As with other figures in this paper, there are multiple data points at a particular temperature from a single paper. These different data points are due to a variation in some other parameter, such as impact velocity, surface roughness, or strain rate. While these other parameters certainly account for most of the spread, they must be neglected since suitable data is not available for proper comparison.

Most of the data available in the literature is at –10 °C, but there is very little data for aluminum at this temperature. All data points shown are averaged values that include at least two samples, which reduces the spread in the data. The data shown includes a range of roughness and impact velocities, which have a pronounced effect on the data. These averaged values range from 27 to 122 kPa for aluminum and from 10 to 494 kPa for steel, where the larger range in steel is due to the increased number of data points from AERTS tests and likely also attributable to a range of surface roughness. In the overall data, there

appears to be a slight trend showing an increase in adhesion strength with a decrease in temperature, but the relationship is not clear. In general, the centrifuge tests have low scatter compared to other tests methods, possibly due to the exclusive use of ice formed from droplet impact. The average scatter for steel is 14.5%, for which all data points were obtained from the AERTS and 21.2% for aluminum. The average scatter was calculated to give even weight to each data point irrespective of the number of repeats at each data point. For aluminum, the average scatter for the calculated centrifuge test was 30.8% and 14.7% for standard CATs. It is worth noting that the CATs and CAT-NGs presented in Fortin et al. [70] contained 337 and 95 points, respectively, and had a standard deviation of 13.3% and 16.6%, respectively (unfiltered, Fortin et al. also filtered the data to exclude erroneous data points and reduce scatter, which is excluded here).

The only parametric studies with a significant number of data points conducted using a centrifuge apparatus come from the AERTS facility. Soltis et al. [47] found that, in general, the adhesion strength increased nearly linearly with decreasing temperature, however, this is likely partially due to an increase in stress concentration at the interface due to a shift to glaze ice, which would result in a lower apparent adhesion (see Fig. 4). It is unlikely that the variation in shape accounts for the entire relationship since other authors report a similar trend when they have no such variation in shape [118]. Tarquini et al. [46] and Soltis et al. found increasing adhesion strength with increasing roughness, though the relationship was less clear (see Fig. 7(b)). Interestingly, the spread in the data is shown to increase with increasing roughness, shown in Fig. 7(a).

2.2 Common Direct Mechanical Tests

While the most data produced by a single group almost certainly comes via the centrifuge test, most authors use direct mechanical test methods. The two common direct mechanical test methods are the push (or pull) test and the shear test. A push test is defined as a test for adhesion in which the interface is broken via a force created from a loading on one side of the sample. These tests are not designed to create a uniform stress at the interface. A shear test is defined as a test in which the load is distributed over the ice sample in an apparently uniform manner, meant to distribute force evenly at the interface. Neither test method is capable of creating a uniform shear stress at the interface, nor do many authors with test data in both groups correct their data using FEA. Several tests using the direct application of force to the ice sample do not fit into this section and because they are not commonly used, this distinction is merely made for convenience herein.

2.2.1 Push Test Methods

Push tests represent the most diverse category of tests performed to test the adhesion of ice. For nonimpact ice, push tests are very straightforward: ice can be frozen to a substrate using a mold, the mold can be left in place or removed, and the ice is pushed or pulled using a force probe. The archetypical paper for most of the recent papers using this method is reference [19], other papers include references [16, 17, 80-83, 86-88, 90, 96-98, 100, 104, 121]. Other test geometries have been used, including an early set of tests pulling

molds with a string [72-74], pushing droplets with a needle [85, 103], a washer on a cylinder (used in a warm environment) [93], and others [9, 75, 77, 84, 89, 94, 95, 101, 121]. Push tests on nonimpact ice are discussed in the next section.

2.2.1.1 Push Tests on Nonimpact Ice

There are few conceptual problems with push tests in a mold for nonimpact ice, in fact the primary problem with these methods is that they cannot be applied to impact ice. The next problem is that FEA needs to be performed on the test geometries to correct the data. In Meuler et al., glass cuvettes were used with finely polished edges restricting the geometry of the ice at the edges, and each sample was frozen from the bottom up using a Peltier plate to reduce stresses frozen in the ice [19]. Each sample was then pushed individually off the test surface using a force transducer and a motion stage with a controlled rate of motion. The probe tip was well controlled and the geometry was suitably described such that a reader could compare their results to FEA. Other tests with similar methodology used other materials for cuvettes or an entirely different mold. One particular paper using a similar methodology introduces a new problem by pushing all the samples at once and reporting an "average" result [89]. The problem here is that testing multiple samples at once will bias the data to lower values; once the weakest sample fails, the remainder will see a step increase in force and will be much more likely to fail as well. Saeki et al. used a push test with ice formed in a mold and held under compression [119]. In a paper primarily using shear tests, Terashima also used a push test with mold-formed ice [121]. Their data plots containing information from their push test were ambiguous and data could not be used (this was also true for some of their shear data, see their Fig. 9 to Fig. 11, vertical axis could not be determined to be logarithmic or linear in Fig. 9, and the test method used in Fig. 10 and Fig. 11 was ambiguous). Makkonen ran push tests on ice formed in a mold using a belt [9], and his paper is not only notable for including FEA results on stress at the interface, but also for what is perhaps the best discussion of the relationship between hydrophobicity and low ice adhesion in the literature. It is clear from his FEA results that the pusher creates a strong stress concentration along the interface (see Fig. 8).

Several papers using nonimpact ice are also worth mentioning. Bascom et al. used a push test to investigate the adhesive shear strength of ice on steel and plastics, showing a poor correlation with the contact angle [76]. Their work included detailed surface replications of the fracture surface and showed the presence of bubbles at the interface, as well as mixed failure cases and even the grain structure of the ice. An earlier work from some of the same authors looked at the adhesion of ice formed while submerged in oils [75]. Chen et al. [81] authored a more recent paper with interesting results relating to hydrophobicity. Using surfaces with fine micro-pillars, they chemically varied the hydrophobicity without changing the roughness of the surface and showed that the hydrophobicity had little resultant effect on the shear strength of the ice. However, it is possible that the breaking occurred at the interface and the repeated geometry may have

caused the same amount of cohesive breaking while the shear adhesive strength from the top of the pillars may have been negligible.

2.2.1.2 Push Tests on Impact Ice

Using a push test on impact ice is more difficult. Authors have grown ice on an airfoil, cut the ice to partition a sample out of the larger ice shape, and then pushed the ice across the interface using a force probe [10] or placed a complete airfoil into a mold where the mold pushes the ice off [91]. Similarly, ice was grown on a cylinder and a disc was used to push the ice off [11, 78, 79]. Most recently, ice was grown on a rail against a pushing element (see Fig. 9) [92]. In 2003, to obtain the force to remove an ice accretion, but not the adhesive strength, ice was pulled from the leading edge of an airfoil using modified vice grips [99]. The most notable set of push tests on impact ice are those done by Scavuzzo and Chu, who published nearly 200 data points from tests run in the IRT using a set of cylinders where an outer cylinder had a window allowing ice to form on an inner cylinder [48]. In their test, the outer cylinder would then be rotated with respect to the inner cylinder to remove the ice (see Fig. 10).

There are several predominant issues common to most push tests used on impact ice. The first issue is that they all use different geometry, making comparison difficult. This is exacerbated by the fact that only one of these used FEA to investigate their results (Lou et al., [92]). The authors of this paper were unable to find the source of material properties presented in Table 1 in Lou et al.'s paper [92]. The simulation provided by Lou et al. deserves some attention since simplified geometry was used, potentially missing stress concentrations from the shape of the ice near the edges of their geometry. While their paper is likely the best example of what a paper presenting adhesion data on ice should look like, they do not provide sufficient data on their icing cloud, and the test geometry will have highly irregular collection efficiency. The same can be said of Scavuzzo and Chu's paper; sharp edges around the adhesive test area lead to highly variable collection efficiency and strong stress concentrations [48]. Unfortunately, Lou et al. did not provide many data points, and data on the scatter from their tests was not available.

One important concept from Scavuzzo's and Chu's as well as Lou's work is to have the pushing element present when growing ice, such that ice grows naturally between the substrate and the pushing element, to reduce the amount of handling required. While Lou's work is a true in situ experiment, Scavuzzo and Chu's involved some handling as samples were moved to the shear rig downstream in the tunnel. Giving equal weight regardless of the number of repeats, Scavuzzo and Chu's data had an average standard deviation of 24.6% for aluminum and 15.9% for steel. Interestingly, Scavuzzo and Chu overreported their average standard deviation at 42% [48], likely because they grouped tests together irrespective of certain variables. To examine this more closely, the standard deviation for their data was calculated in two other ways. Averaging all repeats and averaging the standard deviation of each data point yields an average standard deviation of 21.6% for aluminum and 13.2% for steel. This process was repeated, except that the standard

deviation of each data point was multiplied by the number of repeats at that data point and averaged using the total number of repeats for the data set; this yielded average standard deviations of 23.0% for aluminum and 15.2% for steel. Scavuzzo and Chu's paper is perhaps the most important paper providing data on the adhesion of aircraft ice and is widely cited and used for comparison. Scavuzzo and Chu commented that the scatter was likely inherent to the measurement of ice adhesion. They mentioned that careful surface preparations and repeatable conditions in the tunnel are necessary for more accurate measurements.

The work of Druez et al. is also worth mentioning since theirs is the only parametric study where the microstructure of the ice was reported [78, 79] (their push tests were based on that by Phan et al., [11]). At speeds of up to 23.5 m/s, they showed that the impact velocity, temperature, and cloud properties had a significant effect on the grain size of the ice produced. Since the bulk properties of ice depend on the grain structure, it is possible that the grain structure influences the stress concentration in all tests and may be a good measure for the adhesion strength of ice. This also has implications for FEA on ice, which is necessary to obtain the stress concentration in an adhesion test. However, little data is available on this apart from these works by Druez et al. In these works, ice was grown on cylindrical aluminum bars (conductors) that were machined on a lathe, and a washer-shaped ring was used to push the ice off. However, like others' work, the stress concentration was unknown. Furthermore, these tests were conducted at speeds too low to be directly relevant to aircraft icing.

At least two authors have run push-type tests on airfoils. Merkle ran a push-type test in the IRT by running a traditional icing test where ice is grown on the leading edge of an airfoil and then a patch of ice is cut out with a steam gun [10]. The patch of ice was then pushed off the leading edge of the airfoil with a force probe. This test is a particularly interesting work because it is not only one of the earliest adhesion tests conducted in the IRT (in 1968), but also it tested Teflon® surfaces under impact conditions. Merkle's results, as well as others, highlight the fact that droplet momentum is critical to the adhesion strength for surfaces that depend on the Cassie-Baxter wetting state to reduce adhesion. Merkle's results indicate that studies using nonimpact or low-speed impact tests may not be relevant to aircraft icing [12, 107, 124]. Highlighting this difference between impact ice and nonimpact ice was a primary objective of Merkle's test. Merkle noted difficulty with temperature control during the tests since the tunnel velocity drop prevented the facility from maintaining temperature. Merkle also made a series of observations as to potential sources of uncertainty in ice adhesion measurements, such as variations in the stress concentration due to the geometry of the ice (noting the ice did not seem to slide off of the interface, but rather popped or peeled off), as well as localized stress concentrations, bubbles, and the crystal structure at the interface. Using a steam gun likely caused issues as well since melted water or frozen steam could change the characteristics of the ice being tested, and like other tests, the stress concentrations were essentially unknown.

The other push test performed on an airfoil was that by Kraj et al. [91]. In their test, a short airfoil section was iced, and the edges can be seen to have a large effect on the shape of the ice in their paper. The airfoil was removed from the tunnel and placed above a special fixture molded to the shape of the airfoil, such that the airfoil could be slid into the fixture while ice would be sheared off. This test results in strong stress concentrations, and as the ice geometry varied significantly, these concentrations likely varied between runs. This is a good example of the effect of sharp edges on the collection efficiency of samples in an icing cloud. The extracted results from all push test papers found with repeat tests on aluminum, steel, or Teflon® are shown in Fig. 11 and Fig. 12.

2.2.1.3 Push Test Data

Similar to the CAT results, the push test results show an increase in adhesion strength with a decrease in temperature. The large number of data points at different test conditions and from different test methods produces a wide scatter in the data in a range similar to that for the CATs. The average standard deviation for all push tests was 23.9% for aluminum, 15.1% for steel, and the single data point for Teflon® had a standard deviation of 52.4%. The value for steel is close to that of Scavuzzo and Chu since their data makes up the bulk of that data set. Without the data from their 1987 paper, the average standard deviation for all other papers was 23.7% for aluminum and 10.8% for steel. The values are likely higher for Scavuzzo and Chu since they used impact ice, and most of the remaining data comes from ice formed in a mold. It is worth nothing that the standard deviation appears to increase with increased temperature.

When compared to the year of publication, the standard deviation does not follow an obvious trend (see Fig. 13). The more recent push tests have good scatter, the earlier tests also report good scatter, but tests between 1968 and 1996 report a wide range of scatter; in most cases this is likely due to the larger sample sizes tested. No improvement in scatter can be related to the date of publication or improved test methods. The results from the two papers with the largest data sets are explored in greater detail. Scavuzzo and Chu's data is shown independently in Fig. 14. Data from Druez et al. is shown in Fig. 15.

Scavuzzo and Chu's data for aluminum shows a strong trend with temperature, showing increasing shear strength with decreasing temperature. In general, the thickness of their samples appears to have an inverse relationship with strength, possibly due to higher stress concentrations present in those samples. Increased velocity also showed an increase in adhesion strength. The data for steel is not so clear. From a visual inspection, increasing velocity tends to show increasing shear strength (notice the higher concentration of large markers near the top of Fig. 14(b)), but the trend is not clearly represented in the data. At low temperatures, Scavuzzo and Chu interpreted the data for steel to show a linear increase in strength for data points between 0 to –8 °C and a flat trend from –8 °C and below. There is no obvious relationship between the thickness and strength for steel. Thicker samples seem to be concentrated in the center (red markers), contradicting the data for aluminum. While data is plotted by temperature and organized by velocity and thickness, the data

points are plotted irrespective of the tunnel properties and test geometry. Several data series contain multiple data points because of this (where each data point shown in Fig. 14 is an averaged value). Grouping these points together likely explains the higher scatter reported by Scavuzzo and Chu, as previously discussed. Anderson and Reich later reused the same test rig and commented that the cylinders were prone to freezing together while the required handling destroyed samples for a number of surfaces in their tests (primarily with low-adhesion surfaces) [27]. Anderson and Reich's work focused on nontraditional materials, and their data only contained a small number of data points for aluminum, which were excluded from this paper.

Druez et al.'s 1986 data shows a nearly linear increase in adhesion strength with decreasing temperature for warmer temperatures and either a flat or an opposite trend for lower temperatures, with the only exception being the lowest velocity case. They also showed that their cloud with higher liquid water content (LWC) and mean volume diameter (MVD), condition B in Fig. 15, generally resulted in much higher adhesion strength, especially at lower temperatures, again with the exception of the lowest velocity tested. They reported an average standard deviation of 27.0%. This trend, similar to that reported later by Scavuzzo and Chu for steel [48], may be due to a transition from adhesive to cohesive failure [118]. This may be the case since the increase in adhesive strength may exceed the cohesive strength once the temperature drops below a certain point. This may not have been observed by Druez. et al. and Scavuzzo et al. since the transition may have been on the scale of the roughness elements in the surface; the authors of this paper have found no data in the literature to confirm or deny this possibility. However, Raraty et al. suggest this may have been the cause of a similar trend in their data [118] and no authors in the literature reported looking for this or would even have been able to because of contamination of the surface due to sublimation or deposition.

2.2.2 Shear Test Methods

While there are less shear test publications than push or centrifuge test publications, it is worth noting that many of these papers contain detailed discussions regarding fundamental problems to measuring ice adhesion and they are an excellent resource of literature in this regard. Raraty and Tabor's paper [118] is still commonly cited nearly 60 years later and is the only work known to the authors of this paper to have tested adhesion on an atomically flat surface (using mica). They discussed a ductile to brittle transition in the ice, the effect of stress concentrations, and are one of few papers to give an explanation of the different trends seen in temperature measurements. Jellinek authored a large set of papers relating to ice adhesion, which contain some of the earliest discussion of the disordered interface (also known as the liquid-like layer or quasi-liquid layer) with respect to ice adhesion [77, 111, 112, 125-128]. Anderson and Reich's works contain excellent discussions of the tests performed in the IRT [27, 30, 129]. Haehnel developed the 0° cone test, which is the only commercially available ice adhesion tester known to the authors of this paper [130], and was one of the earliest works including FEA on their analysis [110]. Makkonen recently

published data showing stress concentrations from thermal expansion in the 0° cone test [9].

Shear tests can be generally categorized as having one of three basic geometries: the lap-joint geometry, where two flat plates sandwich ice together [6, 7, 26, 27, 105, 106, 109, 111-115, 129], the 0° cone test and similar geometries [8, 13, 107, 108, 110, 117, 120, 122, 131]; and rotational shear geometries (see Fig. 16 [116, 118]). The rotating shear tests involve forming ice in a mold, attaching it to a base, and then attaching it to a rotating device. The rotating device is then twisted to break the adhesion between the ice and the rotator. No shear tests were found to use high-speed impact ice; all tests either used a low-speed spray, or, as in the vast majority of cases, water poured into a mold and frozen. This is because the geometry used in all current and past shear tests is problematic for the growth of impact ice. These tests are included in this paper since these test methods could be adapted for use on aircraft ice either by modifying the geometry or refreezing the surface of the ice away from the ice-substrate interface.

2.2.2.1 Rotational Shear Tests

Raraty and Tabor used two different types of rotating shear apparatus: a cylindrical apparatus, and an annular apparatus (see Fig. 16). They also performed tests using a frictional apparatus [118]. Petrenko also recently used a similar annular apparatus [116]. The cylinder apparatus used a baseplate with a lip at the edge, on which a cylindrical specimen was set. Water was then deposited to bridge the area between the base and the cylinder. This likely had high stress concentrations in the ice at the point where the base met the specimen, which was not accounted for in their data. These apparently high concentrations make it difficult to classify this test, but it was included with the shear tests since the accompanying annular test was clearly a shear test. The stress concentrations should have been less pronounced in the annular apparatus, which would return higher values for shear strength (though they would not be eliminated as suggested by Raraty and Tabor). A linear trend was observed showing increasing adhesion strength with decreasing temperature using the cylindrical model with the higher stress concentration. With the lower stress concentrations in the annular case, a linear trend was observed from –7 to –10 °C, and at lower temperatures, a flat trend independent of temperature was observed. In this latter temperature range, the ice could be seen to crack cohesively at approximately 45° to the interface. They speculated ductile-to-brittle transition and it was noted that the flat adhesive strength was likely limited by the cohesive strength of the ice. They also observed a linear relationship with increasing adhesion and decreasing temperature on a monolayer of stearic acid (this was postulated to be a result of the stearic acid monolayer only covering part of the surface, also mentioned in [129]), silvered surfaces, and a surface refluxed in benzene. This linear trend was not universal for all surfaces or types of ice tested even when cohesive failure was not present. Using a dilute solution of ammonium chloride, they showed a near step increase below the eutectic temperature and a large, sudden increase in the adhesion of a dilute solution of Teepol on stainless steel below –24 °C (see [118] for

this data). Adhesion of ice to polytetrafluoroethylene (PTFE), polystyrene, Perspex® (Lucite International), and a thick layer of stearic acid were depicted graphically to asymptotically approach a maximum value with decreasing temperature. It is also worth noting that recent researchers have begun presenting adhesion data as a linear fit to their data using a variety of metals following Raraty and Tabor [47]. The frictional method Raraty and Tabor used involved depressing a hemispherical metal tip into ice and dragging the ice under the tip, from which they showed the same linear trend in the data relating temperature and adhesion, albeit with higher values than for their other tests. They based the concept of their shear test on the idea that metals in sliding contact adhere, and the friction is the primary force required to shear the junctions formed. However, it is not clear if this is due to bonding of the interfaces or mechanical interlocking. In either scenario, Raraty and Tabor describe the shearing as occurring in the weaker metal, indicating a cohesive failure inside the weaker material near the interface. This is consistent with Merkle's hypothesis as well [10]. The authors of this paper were unable to find evidence in the literature with which to discern the scenario Raraty and Tabor present; new investigations into the shearing of ice at the interface could likely provide valuable insight into the adhesion of ice.

2.2.2.2 Lap Shear Tests

The lap shear test is the most common type of shear test. Early works include those by Jellinek [111, 112] and Ford and Nichols [6, 132]. These tests appear to have the apparent advantage of having an extremely low stress concentration, however this is not accurate [26, 133]. A number of variations on this test are provided in the literature. For example, Minsk ran tests using a fixture with a linear slide to reduce out of plane forces [7], and a more recently published master's thesis includes double lap shear tests on ice [109]. Andersson et al. used a cord wrapped around a disk to distribute stress in a lap-shear geometry (this paper is close to being considered a push test, but is considered a lap shear test since the pushing element is on a disk instead of the ice) [106]. One advantage that regular lap tests have over the 0° cone test is that the regular lap test enables the ice to expand or contract between the plates, though thermal stresses from forming the ice may still be problematic.

Oksanen used a double-lap shear method to measure the adhesion strength of ice, where the sample material was attached to either side of a steel plate and ice was attached to the samples on either side. They used computer programs to calculate the stress concentration in the ice and found strong concentrations at the edges. Their data was not included in this paper, but it is worth noting they calculated the effect of the strain rate on the adhesion strength of ice and compared it to prior results by Parameswaran [43], as shown in Fig. 17.

Oksanen's paper includes much valuable discussion, but it is also one of few sources of data on the friction of ice. The age of Oksanen's work is shown through some of the discussion on the disordered interface (or liquid-like layer) of ice where the layer is stated to be solely due to frictional heating, where newer theories gives several alternatives [134],

and the properties of the layer are still poorly understood [135]. However, Oksanen's paper possibly makes the strongest argument for the importance of controlling and reporting the strain rate in adhesion tests.

2.2.2.3 0° Cone Test and Similar Methods

The 0° cone test is similar to a lap shear test, except that an annulus and a cylinder are used to shear the ice instead of flat specimens. The earliest version of this test found was by Haehnel and Mulherin, who included FEA stress analysis (see Fig. 18) [110]. This method was used by the same group in several other publications as well [8, 131]. In the 0° cone test, a hollow cylinder forms an annulus around a filled cylindrical rod. The region between the rod and hollow cylinder is filled with ice adhered to both surfaces, and the test is completed on a universal tester by pushing the inner cylinder out along the common axis with the annulus immobilized. Similar geometries involve inserting a cylinder of metal into a large piece of ice and either twisting, pushing, or pulling the cylinder out [108, 121]. The difference in the loading method used by the similar geometries is expected to produce different stress concentrations.

As seen in Fig. 18(a), there are sharp concentrations in the normal and shear stresses near the edges of the ice. It is unclear whether more recent publications took this stress concentration into account [13, 107, 117, 120, 122]. Petrenko and Qi used a highly customized geometry and likely had significantly different stress concentrations [117]. They reported annealing their ice for 48 h; however, this likely aided in reducing stress frozen into the ice during the freezing process. Other authors probably neglected these frozen stresses, however, Makkonen demonstrated later that this stress may have been enough to pre-crack the interface (see Fig. 19) [9].

2.2.2.4 Shear Test Data

The data taken from the literature for shear-type tests are shown in Fig. 20 and Fig. 21. Data for Teflon® and polyurethane are included with the shear test results in addition to aluminum and steel (Teflon® was included in the push test results and polyurethane is also included in the miscellaneous test results). Polyurethane is included since it has relevance to pneumatic deicers, and Teflon® is included since it is a commonly suggested material to use as a low-ice-adhesion surface.

Similar to the data previously discussed, the shear data shows a trend of increasing adhesion strength with decreasing temperature. For steel, the trend appears to follow until around –5 °C, below which a flat trend is observed. The data for aluminum is sparse with shear tests and very little is available for Teflon® or polyurethane. Interestingly, the spread in the data for steel spans over three orders of magnitude, one order of magnitude more than for push or centrifuge tests. Values also tend to read higher (at least at temperatures below –3 °C), likely due to lower stress concentrations in these tests (see Fig. 5 and Fig. 11).

The average standard deviation for Teflon® was extremely high at 136.1%, with one reported value at 300%. The average standard deviation was 11.8% for aluminum, 22.2% for steel, and 27.9% for polyurethane. The 0° cone test data is presented in Table 1 with the values for all methods combined, which shows a significant improvement in scatter over other methods. The high scatter in the Teflon® data was likely a result of the lower adhesion values and from variation in the formation process for the ice penetrating water into the surface elements. With lower adhesion strength, problems like thermal expansion are more likely to pre-crack the interface. Very little data was available in the literature for parametric studies; the two available data sets are shown in Fig. 22.

Susoff et al. found that increasing roughness led to an increase in adhesion strength [120], a trend commonly reported in the literature. Less commonly reported is the relationship between the strain rate in the test and the adhesion strength since most authors test at a single strain rate. Haehnel and Mulherin found that the strain rate had a strong effect on the adhesion strength, where faster tests had a higher adhesion strength [110]. This has strong implications for other tests, especially since few papers report their strain rates and the strain rates present due to stress concentrations may vary locally. In agreement with Haehnel and Mulherin, Oksanen states that the adhesion strength of the ice is strongly influenced by creep in the ice, and that the strain rate affects the adhesion strength because of creep [26].

Raraty and Tabor showed a linear increase in adhesion strength with decreasing temperature (Fig. 23). This trend was not uniform; they noted that for their annular test on steel the data plateaued, taking the points below –7 °C to be linearly decreasing. However, with the fit line added, it appears that the linear trend continued but was flatter than for other test sets (including some not plotted here). The cylinder data and stearic acid annular data (with a poor fit) exhibited linear trends crossing the zero axis at a negative temperature. The trend line for annular test data on clean steel crossed the zero axis at a positive temperature. It is worth noting that their frictional test results had a good linear fit and crossed zero at a negative temperature. They suggested that the data was linear to approximately –7 °C and flat afterwards due to the adhesion strength being exceeded and cohesive breaking dominating at the lower temperatures. Their data were not included in Fig. 21 since no tests were repeated. Raraty and Tabor also showed a dependence on the ice thickness in their data, which is not included in this report.

2.3 Miscellaneous

While the bulk of all tests done on ice adhesion fit into one of the previously discussed categories, there are a wide variety of tests that do not. As previously mentioned, this category includes tension (mode 1) [5, 13, 101, 122, 136-139], pre-cracked tension (where the “crack” is used as a stress riser) [140], cantilevered beam [141-143], torsioned beam [143], tensioned beam [143], four-point bending beam [144], blister (mode 1) [124, 145-150], laser spallation [151], and vibrating beam [152-155]. Several of these tests, the tension tests (including pre-cracked) and the tensioned/torsioned/cantilevered/four-point

bending beam tests, could be considered direct mechanical tests, where a stress-strain curve is produced. Indirect tests include the blister, laser spallation, and vibrating beam tests.

2.3.1 Tension Tests

Tension tests are unique compared to other methods since they are designed to produce a mode 1 tension failure in a direct mechanical, as opposed to the mode 2 shear failure produced from all other tests (except for the blister test). The earliest paper found showing a method to test ice adhesion is a tension test by Rothrick et al. [5]. Rothrick's paper does not contain suitable data for comparison, but contains pictures from their tests. An example test specimen is shown in Fig. 24.

As in all other tests, stress concentrations invariably exist at the interface due to the difference in Young's modulus and Poisson's ratio between the two materials. Unfortunately, no papers were found that provided realistic stress concentrations for this test geometry. These tests have been performed exclusively with ice formed in a mold. More recently, Lee used a similar configuration to test the adhesion of ice with different levels of contamination that used holes similar to Rothrick's for alignment [139]. Other authors have used spring gauges for a fast pull-off test [136, 137]. A notable variation on this test is the practice of pre-cracking the interface and pulling it from one side to produce a known stress concentration. However, no data produced using this method was found in the literature and no information could be found on the stress analysis used for this test [140].

2.3.2 Beam Tests

A number of tests on ice have been performed on beam substrates that were deformed to stress the ice-substrate interface. The most common of these tests are the cantilevered and the vibrating beam tests. The reported work of the cantilevered beam tests was all produced by AMIL [141-143]. In the earliest work referenced in this paper, Blackburn et al. calculated the neutral axis of the ice-substrate beam using classical beam theory, which does not account for stress concentrations at the edges or mismatches in material properties. A similar problem exists with the torsion test and tensioned beam test performed by AMIL [143]. Later, Riahi used a tension beam test and accounted for the stress concentrations at the interface using FEA simulations and a cohesive zone method to investigate crack propagation and found strong concentrations prior to crack formation [156]. Because Riahi used a simplified geometry and a coarse grid, his results may include some questionable stress concentrations. Advanced simulations with better handling of stress concentrations would likely provide useful insight into these test methods. An example of Riahi's results are shown in Fig. 25.

The drawback of beam tests is that the use of a metal substrate dictates the use of higher capacity load cells than would otherwise be needed. However, Laforte and Laforte calculated the uncertainty of their experiments and found it to be smaller than the scatter typical to ice adhesion tests [143]. All authors using these tests had numerous mixed

failures as well. However, there are several potential advantages to these tests for use with impact ice. Unlike other direct mechanical test methods, this test uses open-faced geometry, allowing ice growth matching relevant conditions. Similar to push tests and shear tests, the samples in beam tests are preserved, allowing for investigation. A stress-strain curve is also produced, which allows for better matching against FEA as compared with methods like the centrifuge test. Javan-Mashmool et al. noted that controlling the exact position of the neutral axis is difficult and likely leads to inaccuracies [154].

Javan-Mashmool et al. instead proposed a method using an embedded sensor to monitor the stress at the interface with a vibrating beam. Polyvinylidene fluoride (PVDF) piezoelectric sensors were attached to the interface to monitor the stress, which provided a charge proportional to the induced stress at the interface. They assumed the stress across the width of the beam was constant and varied along the length of the beam and used three PVDF strips to take measurements. They also argued that the modification to the mechanical state of the interface was only modified slightly because of the presence of the strips. However, this is unlikely to be the case because of the importance of roughness and different surface chemistry; the PDVF films likely created stress concentrations at the interface. Further, given the stress concentrations found in the nondynamic cantilevered beam case by Riahi [156], concentrations are likely to have existed in Javan-Mashmool et al.'s test as well. Further, Javan-Mashmool et al. justify the use of their tests by comparison to data in the literature that they suggest earlier is flawed, stating their test is within an order of magnitude. The mean value they obtained was 285 ±67 kPa (or 23.5%), which is in the middle or at the lower end of values obtained by other authors. Generally speaking, because tests with lower stress concentrations should report higher values of adhesion strength, it is likely that these tests had relatively high stress concentrations. The presence of stress concentrations in a similar test was confirmed by Hassan et al., who later performed FEA on a vibrating, composite ice-aluminum interface (though the effects of the sensors were not included, see Fig. 26) [152]. A later work from some of the same authors also used FEA for comparison and included a PVDF strip in the simulation, though they used a low number of elements [155]. It was not clear in either simulation if grid sensitivity analysis was performed, and a lack of refinement near the edges could mask existing stress concentrations. Hassan reported stress concentrations at the edge (located near their strain gauge) and commented on a wide range of concentrations, though it is unclear if this was used to correct the data. Akitegetse et al. showed good agreement between their simulation and their experimental results using a tensioned beam [155].

Hassan et al. updated the method to use a single strain gauge, providing a low-cost alternative to the PVDF sensor. They were able to show a strong correlation between adhesion strength and roughness and were careful to avoid placing the strain gauge between the ice and the aluminum. Their paper contains some helpful discussion on the state of stress at the interface for this method. Strobl et al. authored the most recent paper found to

use a vibrating beam apparatus [153]. One problem with the background information presented by Strobl et al. is as follows:

> *"However, within these previous studies, the ice was frozen on the metal substrates in a non-supercooled state. As covered by this research, the water is frozen onto the specimens by means of a spraying procedure which is comparable to the process of atmospheric ice accretion on aircraft structures."*

This statement was incorrect; one of the papers they cited prior to making this statement was that by Akitegetse et al. (previously discussed) who used a spray system similar to Strobl et al.'s and reported supercooled droplets [155] (although it is unclear in both papers how they verified their droplets were supercooled). It is important to stress that low-speed impact accretions are not comparable to ice formation in aircraft icing; the higher impact velocities found in aircraft icing directly influence the adhesion of the ice, especially with surfaces depending on Cassie-Baxter wetting to reduce ice adhesion (previously discussed in more detail). Furthermore, as Strobl et al. state, they likely obtained polycrystalline ice, but the size of the grains was not recorded (as is typical for adhesion tests) and generic properties for polycrystalline ice were used, which makes the properties used for calculations questionable (as is the case with other papers).

For impact ice, the substrate geometries described for cantilevered and vibrating beam test methods are problematic since the sharp edges presented in these geometries will lead to a higher water collection efficiency. These tests may be adaptable to geometry more suitable to aircraft icing, however, extensive FEA would be required. A more significant problem with the vibrating tests is that the induced stress and strain at the interface is complicated since the strain rate is critical to the measurement of ice adhesion (see Fig. 22).

The last method discussed using classical beam theory to predict adhesion properties is a four-point bending method [144]. Wei et al. used Euler-Bernoulli (classical) beam theory to determine the critical interface fracture energy, as opposed to an adhesion strength, and observed unstable crack bursting. They used a hand saw to cut the ice to produce a notch. They also performed surface replication using Formvar (see Fig. 27), which they noted both etched and replicated the surfaces. Potential problems from their test include a lack of information on the stress concentrations and the possibility of damaging the sample while sawing.

They performed tests with polycrystalline ice and a single crystal of ice and found a strong dependence on the type of ice used and the interfacial fracture energy (fine polycrystalline, 1 J/m^2; tap water, 4.5 J/m^2; single crystal, 19.2 J/m^2). This also had a visible result in their surface replications. Each case had a mixed adhesive and/or cohesive failure, shown with a good level of detail in their surface replications. Whether cohesive breaking occurred on the size scale of the roughness elements was not apparent to the authors of this paper, and it is likely this information was not preserved because of the effect of etching.

2.3.3 The Blister Test

An example blister test apparatus is shown in Fig. 28. In the blister test, a disk with a hole in it is iced over the top, typically using a spray nozzle. The edges near the hole are covered prior to icing with a small disk of specified thickness to create an artificial defect, acting as a stress riser. The hole, covered by ice, is pressurized until the ice cracks and separates. Adhesive, cohesive, or mixed [157] failures may occur. The ice fracture energy is then calculated as a function of the pressure to remove the ice and the geometry of the test. The first paper using the method was published in 1969 [157], though the method was not used on ice until 1983 [147]. The blister test has several advantages. First, the method is one of very few designed to provide mode 1 interfacial strength. Second, this method can be conducted using inexpensive hardware. Third, the design uses simple geometry, which could likely be adapted for a variety of geometries. Last, a small modification adjusts the test to provide cohesive strength data or adhesive strength data. Disadvantages include the inability to produce a stress strain curve and possible variations in stress concentrations due to either imperfections in the ice or the thickness of the disk used to create a defect.

2.3.4 Laser Spallation

The laser spallation technique only appears in one publication by Archer and Gupta [151]. In their test, a pressure wave was created on an iced substrate by heating the back side of the substrate with a laser. The magnitude of the pressure wave was controlled with the heat delivered from the laser. FEA was used to determine the resultant stress at the interface from the laser-induced pressure wave. In a given test, the laser was pulsed using increasing energy until the ice interface visibly cracked. While they reported very low values of standard deviation (averaging 4.9%), they did not report standard deviations for all tests and, more obviously, their data is roughly two orders of magnitude higher than any other data in the literature. While their method may have had very low stress concentrations due to the geometry of the test, based on the stress concentrations reported by other authors, this is not enough to explain their abnormally high values of adhesion strength [25].

2.3.5 Peel Tests

Only one paper by Scavuzzo and Chu was found presenting results from peel tests [48], which did not contain data suitable to include in this report. Peel tests provide mode 1 failure results, though, like all other test methods, suffer from stress concentrations at the interface. These stress concentrations are certainly strongly dependent on the materials used, but have several important benefits. They can be used with impact ice, as demonstrated by Scavuzzo and Chu, and since ice grows on top of the substrate, they should provide results independent of the complex surface geometry that most aircraft ice exhibits. No FEA is known to exist to examine the stress concentrations in these tests. The geometry Scavuzzo and Chu used can be seen in Fig. 10(a), next to their push type test. Their test used a complex internal pulley system to perform the test.

2.3.6 Miscellaneous Test Data

Very little parametric data is available in the literature from tests in this category. Laforte and Laforte found decreasing adhesion strength with increasing sample thickness for two of their three test methods (tensioned and torsioned beam), though the cantilevered beam results were mixed [143]. Strobl reported decreasing adhesion strength with increasing contact angle [153], and Yeong et al. reported mixed results relating the fracture energy and the contact angle [149]. Hassan's results comparing roughness to adhesion strength are shown in Fig. 29. The "bad" data point was used in place of the presented data in other figures since no suitable reason could be determined to exclude the data for that point. Similar to the data shown in Fig. 22, the adhesion strength is reported to increase with increasing roughness, though in this case the trend line crosses zero before zero roughness is reached.

From the data shown in Fig. 30, it appears that adhesion strength increases with decreasing temperature. Comparatively, the laser spallation tests had extremely high values of adhesion strength with extremely low deviation. The scatter in the data covers a wide range, as shown in Fig. 31. Some scatter reported by Laforte and Laforte is suspected to have been overreported since it is well above 100%. The affected values are shown with and without this data point in Table 2. The average standard deviations of the methods in this section are shown in Table 2.

3 Discussion

Data used for all plots (and some that have been omitted) are shown in the supplemental material. The scatter in the literature has been shown for individual tests previously mentioned and averaged for each category of tests. In gathering data for comparison, data were excluded if the standard deviation was not available (with the exception of Fig. 23). In some cases, the standard deviation was reported but the number of samples was not. Since two repeats were considered enough for inclusion, the standard deviation was plotted against the number of repeats at a data point to determine if lower sample sizes resulted in significantly different values of standard deviation. These are shown in Fig. 32 and Fig. 33.

The data for aluminum did not show a significant increase in scatter compared with the number of repeats. For steel, there appears to have been a small upward trend for data points with less than five repeats. A statistical analysis of a set of data points containing a large number of repeats would provide useful information on the scatter inherent to adhesion testing. This is currently only available for the CAT method, where data unfortunately had varying strain rates [70].

Valuable test methods are ones that provide accurate and precise results. The standard deviation provides a measure of precision, but there is no good way to measure the accuracy of a test without a true value. Across all tests, there was an average standard deviation of 24.5% for aluminum, 17.2% for steel, 24.2% for polyurethane, and 124% for Teflon®, with 21.2% if the data from aluminum, steel, and polyurethane were combined.

For example, if comparing by precision alone, laser spallation would appear to be one of the best techniques available, yet when compared to the other available data suggests that the laser spallation data is erroneously high. However, the other tests are likely biased to yield low values of adhesion since the stress concentration on the interface is frequently ignored, so there is no true value from which to judge the accuracy of the laser spallation test. Because of this, the accuracy of each test method is best discussed in terms of the trends they show, the conceptual problems they have, their precision (standard deviation), and a relative comparison of their data to that of other methods. The precision of tests and relative comparisons are discussed in the previous sections. Conceptual problems are discussed in the Conceptual Problems in the Literature section, and trends in the data are discussed in the Data Trends section. The sections are presented in this order to emphasize the caution that must be taken when considering the data in the literature.

3.1 Conceptual Problems in the Literature

There are many problems with the literature that presents data on ice adhesion. For example, as a general rule, papers that present adhesion test data do not correct their data with stress concentrations, which could result in values an order of magnitude lower than the true adhesion strength [25]. This ensures that competing tests will not compare well since they have different stress concentrations. It may also bias trends in the data. Many authors report higher adhesion of glaze ice, which may be because glaze has a higher adhesion strength. This could also be because certain ice shapes have larger impingement limits, which increases the contact area and disperses stresses to the substrate more evenly. It may be possible that the frozen stresses in a glaze shape are lower than those in a rime shape. Many other problems exist in the literature. Unfortunately, there is now a long history of problematic reporting in the literature as a result of following precedent.

The primary problem in the literature is the issue of stress concentrations; this point is well made by Schulz and Sinapius [25]. The state of stress at the interface is universally nonuniform, but authors almost exclusively ignored this. Of 113 papers compared in this paper reporting experimental data, only eight used FEA and just five of these papers were published after 2009. The earliest simulations were reported in 1998 [110, 151]. Of the 113 papers with experimental data, 83 were published after 1995 and 58 were published after 2009. All these simulations use simplified geometry, and none are known to the authors of this paper to present a grid sensitivity study. In many of the papers with FEA, it is unclear how these results were used to analyze the experimental data.

The simplified geometry is extremely problematic for tests on aircraft ice. From Fig. 4 it is apparent that ice shapes have highly variable geometry. Ice formed from clouds with larger, warmer droplets will have larger impingement limits and more runback than that formed from ice at lower temperatures and smaller droplets, but this can also form horns or scallops. These irregularities change how the ice distributes stress to the interface, causing stress concentrations. Quantitative data cannot be produced with better than one order of magnitude accuracy as long as this is not accounted for. Ultimately, either tests will require

correction using 3D scans of the ice or geometry-independent test methods will need to be created.

The interaction with the surface roughness is also especially problematic. Chen et al. show simulation results that demonstrate the presence of stress concentrations around roughness features, which cannot be characterized with average roughness [158]. This is also discussed by Fortin et al. in the context of developing a model for adhesion [159]. Few papers report critical test parameters, such as the strain rate, contact angle, impact parameters, and surface roughness. More often than not, papers that report one of these values exclude the others. Looking more closely at roughness, it is certain that standard measures of roughness are not sufficient to describe the relationship between roughness geometry and ice, and some authors have started to characterize the surfaces they test with the autocorrelation length [124]. As seen in Fig. 22, the strain rate can have an order of magnitude effect on the apparent adhesion strength. Similarly, roughness also has a large effect. This alone is enough to account for most of the difference in reported adhesion strengths without considering stress concentrations.

Documentation is also particularly poor on the grain structure of the ice under test. To make accurate comparisons, the ice under test should have the same microstructure. It has been shown that the microstructure of the ice is sensitive to the accretion parameters at low speeds [78], but most authors neglect this. This highlights issues with testing in different facilities, where clouds are calibrated differently and may not be equivalent, and the use of different geometry, which will change the collection efficiency and likely change the microstructure of the ice. A comparison of the different types of adhesion test methods reviewed is listed in Table 3.

It may also be important to run materials tests in the tunnel with the cloud still on. The limited discussion of this topic available in the literature suggests that the structure of ice will change as the cloud is turned off since the thermodynamic state changes [160]. When supercooled water accretes on the surface, it releases latent heat into the ice, warming it above ambient conditions. When the cloud is turned off, the ice cools and liquid water in the ice may solidify. As previously discussed, creep is an important factor in the adhesion of ice and affects the adhesion strength as a function of the strain rate the ice experiences. Residual stresses frozen into the ice will also be time dependent, and testing at a particular time of interest after the onset of accretion is likely important for some icing conditions.

Preferred methods should preserve the sample and allow fine control of the strain rate, as well as allow for easy comparison to FEA. Methods with low scatter are also desirable, and given the complex state of strain at the interface, methods should be able to test using variable geometry or configurations to document the difference between mode 1 and mode 2 failure. No test presented in this paper is ideal, and the recommended path forward is to either develop a new test method to address these problems or to use a lap shear test that may be reconfigured into a tension test and simply test a large number of samples. The

primary problem with adapting a lap shear test with impact ice is the need to sandwich the ice. Beam tests are promising and have the advantage of being easier to use with impact ice since the ice does not need to be sandwiched, but the stress state at the interface cannot be varied as readily. While they produce lower-than-average scatter, centrifuge methods are not recommended because of the inherent difficulty in controlling the strain rate, which has been shown to have an order-of-magnitude effect on the strength of the ice, as well as the other disadvantages listed in Table 3. Other tests, like the blister and the laser spallation test, likely require more development before they can be used.

3.2 Data Trends

As previously discussed, there is no conclusive data in the literature such that the adhesion strength for a substrate with a given roughness under a specific ice condition can be identified to within 20% accuracy. The data in the literature generally agrees within two or three orders of magnitude at a given temperature, and data on the roughness and other critical parameters is poor. The value that the data may provide is the identification of certain trends. Trends discussed herein are with regard to the test temperature, impact velocity, contact angle, and roughness. The data for roughness and contact angles are poor, though there is a strong consensus that an increase in roughness leads to an increase in adhesion strength, and an increase in wetting angle leads to a decrease in strength when roughness is not a factor. While trends are present because of other effects, such as creep, these were only present in a small number of individual papers and were previously discussed.

The bulk of the data in the literature comes from recent papers on specialized surfaces that are impossible to compare. Some data exists in the literature for titanium and several alloys, but was only found in two publications [47, 147]. Nylon was another relatively common material, but too few data points were available for comparison [6, 18, 74, 88]. Teflon® and polyurethane are compared with temperature; however, formulations between papers may have been different. As previously mentioned, alloys of steel and aluminum were grouped together with steel and aluminum, respectively. Nearly all data points for polyurethane and Teflon® were run using mold-formed ice, and so these surfaces are not included in the velocity comparison.

3.2.1 Temperature

There is general agreement in the literature that the adhesion strength of ice to arbitrary substrates increases with the decrease in temperature. This is most prominently stated by Raraty and Tabor (see Fig. 23 [118]) and more recently by Soltis et al. (see Fig. 7, [47]). Druez et al. also reported data showing a nearly linear increase at lower temperatures, but the data points at the lowest temperature tested showed little change or even a decrease in adhesion strength, presenting a plateau similar to what Raraty and Tabor saw in their tests (see Fig. 15, [78]). Scavuzzo and Chu reported an increase in strength with decreasing temperature (see Fig. 14, [48]), but linear trend lines poorly represent their data. In their paper, they combined their data and suggested steel and aluminum had similar adhesion

strengths, which gives the appearance of a linear trend at warmer temperatures and a flat trend at lower temperatures in their data. However, Oksanen points out that since the elastic modulus and creep of the ice are highly temperature dependent, the relationship is likely not so straightforward [26]. Furthermore, the substrate properties may be temperature dependent as well. The compiled data for aluminum, steel, polyurethane, and Teflon® is shown against temperature in Fig. 34 to Fig. 36.

The data for aluminum exhibits a weak exponential trend, showing increasing adhesion strength with decreasing temperature. Linear fits were attempted with poorer results; the poor fit of the exponential curve demonstrates the poor agreement of the data. When looking at all the data, the linear trends seen in other papers are obscured. The disagreement over the magnitude of adhesion strength is well highlighted by comparing the data at –10 °C. For all test methods, the data spans three orders of magnitude, approximately four and one-half including the laser spallation data. Steel appears to exhibit a stronger trend, but this is almost entirely due to a single data set at –1.7 °C that returned particularly low values. Above this, the trend is nearly flat. Teflon® and polyurethane may show an increasing trend with decreasing temperature, but the data is not clear, likely due to the lower number of data points. A linear trend was not observed across all papers and the trends reported by various papers differ significantly. While Raraty and Tabor suggest that the plateaus observed in the data may be due to cohesive breaking, there is no conclusive evidence for this. Given the lack of attention paid to stress concentrations and the poor data available for Young's modulus of ice (especially impact ice) as a function of temperature, the apparent relationship with temperature could be entirely due to systematic errors in the data. However, this is thought to be extremely unlikely and the trend in the data is likely due to a physical mechanism not yet understood.

3.2.2 Velocity

Accurate accretion conditions are often neglected when evaluating adhesion strength for aircraft ice. This is best characterized for adhesion by the impact velocity of the water. For water poured into a mold and frozen, the velocity was taken to be zero. Fig. 37 shows the data for aluminum, and Fig. 38 shows the data for steel. Laser spallation data were excluded for aluminum.

In the data for aluminum, a sharp decrease in the maximum observed values occurs when switching from mold poured ice to impact ice. However, at higher speeds, the data remain relatively flat. There is still large variation in the data, ranging from 25 to 661 kPa, with an average of 363 kPa. For mold-formed ice, the data ranged from 152 to 3901 kPa, with an average of 882 kPa (excluding laser spallation data, including those two points raises the average to 13.1 MPa). Data for nonimpact ice on aluminum was taken from 12 publications (37 data points), compared to 14 providing data for impact ice (73 data points). Some possible explanations for the higher strength and variation in mold poured ice are differences in stresses frozen into the ice, larger grains in the poured ice resulting in higher

strength, and weaker stress concentrations at the interface due to a lack of penetration into roughness elements.

In the data for steel, the difference between mold poured and impact ice is much less clear. For impact ice, the measured strength ranges from 10.3 to 856 kPa, with an average of 309 kPa, with 56 data points. For mold-poured ice, the strength ranges from 1.41 to 1410 kPa, with an average of 381 kPa, with 40 data points. The higher scatter for mold poured ice may be due to the data for impact ice on steel coming from a smaller number of papers (3 versus 10).

For both steel and aluminum, the average reported strength (irrespective of duplicates at a data point) was higher for mold poured ice than impact ice. The velocity is expected to have a much stronger impact on surfaces relying on Cassie-Baxter wetting since high impact velocities typically, if not universally, transition wetting on these surfaces to a Wenzel state. However, tests on nonimpact ice are reported to have higher maximum stresses than impact ice for both aluminum and steel and a larger range in reported values.

4 Conclusions

There are many open questions with regard to ice adhesion and the material properties of aircraft ice. How significant are the frozen stresses in the ice, and what is the time sensitivity of testing for relevant icing conditions? When is cohesive breaking present in the roughness elements of a surface? Are there bubbles trapped at the interface? How much of the apparent adhesion strength is due to the interaction of roughness, and how much would be present on an atomically flat surface? What role does the disordered interface (or liquid like layer) play in the adhesion of ice? What are the mechanical properties of aircraft ice away from the interface? Until these and similar questions are answered, it will be difficult or impossible to develop useful models to predict the adhesion strength of ice and to be useful on an aircraft a given surface would have to undergo a tremendous amount of testing to satisfy the unknowns that currently burden the industry. Test methods that preserve the sample geometry are much better positioned to answer these questions as well as test methods that produce stress-strain curves for analysis of the strain rate.

The literature was investigated and 113 papers were found to report performing tests on the adhesion of ice. Papers containing data for aluminum, steel, or Teflon® were selected for comparison and data were collected from 58 papers. Average values of adhesion strength and standard deviations of repeat test points were calculated for comparison of methods. All methods were found to have conceptual problems for application in aircraft icing.

Several parameters have proven to be important and are almost exclusively neglected in the literature, such as the strain rate. The influence of geometry on the stress concentrations at the interface is not largely accounted for, and simulations to account for this use data from nonimpact ice. The literature reports adhesion values for common materials over three

orders of magnitude at a given temperature, and there is no method or suitable data set to use to judge which values of adhesion are accurate for impact ice. Systematic errors in the literature likely bias reported adhesion data to values lower than their true value. No papers report data on all the parameters important to the adhesion of ice.

The literature provides good evidence that increasing roughness results in an increase in adhesion, as does decreasing temperature. These relationships are not strictly clear, however. The relationship between the adhesion of ice and the wetting properties of a substrate are not clear; mixed trends are reported in the literature, especially when using impact ice. There are also a number of open questions in the literature that need to be answered before useful models for adhesion can be created.

Issues in the literature relating to the calibration of clouds used for accreting impact ice were mentioned in passing, though this issue is likely to create a significant variation in data produced between different facilities. Authors of future papers presenting adhesion data are encouraged to provide more detail relating to the calibration of their facilities, finite element analysis (FEA) of their tests, characterizations of surface roughness, and the strain rate at each test point. While this review was intended to capture as many papers from the literature as possible, a number of important papers were not available (as mentioned in the introduction), and many papers are certain to exist of which the authors of this paper were not able to find.

Acknowledgments

The authors wish to thank Eric Kreeger, Dr. Mario Vargas, and Dr. Andy Gyekenyesi for helpful discussions of the literature; Tom Lavelle and Nancy Mieczkowski for their extensive editorial help; the NASA Glenn Library for their support in providing journal papers; Jordan Salkin for her help in finding higher quality images for tests performed in the IRT; and all of the authors who tabulated their results. This work was funded by the NASA Revolutionary Vertical Lift Technology project.

Fig. 1. The Anti-icing Materials International Laboratory's (AMIL's) original Centrifuge Adhesion Test (CAT) setup. (Reprinted with permission from [18], © Caroline Laforte.)

Fig. 2. Finite element analysis (FEA) results for Centrifuge Adhesion Test (CAT) using aluminum beam. (a) Deformation ×200 on aluminum beam, out-of-plane normal stress. (b) Shear stress. (c) Normal stress. (Reprinted with permission from [67], © Heli Koivuluoto.)

Fig. 3. Adverse Environment Rotor Test Stand (AERTS) facility. (a) Schematic of coupon mount. (b) Image of original mount. (c) AERTS stand in 2014. (d) Updated coupon geometry. CF, centripetal force. ((a) and (b) reprinted with permission from [63], © American Helicopter Society International, Inc. (c) and (d) reprinted with permission of AIAA via Copyright Clearance Center from [47], © AIAA Journal by American Institute of Aeronautics and Astronautics, Inc.)

Fig. 4. Ice grown on the AERTS. (a) to (c) Ice samples accreted prior to shedding. (d) to (f) Test coupon after shedding. (g) and (h) Method for area calculation. (Reprinted with permission of AIAA via Copyright Clearance Center from [47], © AIAA Journal by American Institute of Aeronautics and Astronautics, Inc.)

Fig. 5. Adhesion data from centrifuge tests in the literature. ICAT, instrumented Centrifuge Adhesion Test; CAT-NG, Centrifuge Adhesion Test-NG; CCAT, calculated Centrifuge Adhesion Test; st, steel.

Fig. 6. Standard deviations of centrifuge tests in the literature. ICAT, instrumented Centrifuge Adhesion Test; CAT-NG, Centrifuge Adhesion Test-NG; CCAT, calculated Centrifuge Adhesion Test; st, steel.

Fig. 7. Recreated data from [46, 47]. Trend lines added in MS Excel by using same data from Fig. 5. 90° tests run with sample orthogonal to 0° test sample orientation. (a) Temperature data at constant roughness. (b) Roughness data at constant temperature. Dir, direction.

Fig. 8. Shear stress in Makkonen's push test, deformations ×1000. Shear stress is in Pa. (Reprinted with permission of VSP via Copyright Clearance Center from [9], ©2012 Journal of Adhesion Science & Technology by VSP.)

Fig. 9. Rail and pusher in situ experiment. (Reprinted with permission of AIAA via Copyright Clearance Center from [92], © Journal of Aircraft by American Institute of Aeronautics and Astronautics, Inc.)

Fig. 10. Cylinder with window push test and peel test. (a) Front of model, peel test is the large drum on the left side, right is push test coupon mount. (b) Back side of model showing adhesion tester at top left. (c) Square window cylinder mounted in adhesion tester in tunnel, used from [48].

Fig. 11. Adhesion data from push/pull tests in the literature. Cyl., cylinder; Tef., Teflon®; st, steel.

Fig. 12. Standard deviations of push tests in the literature. Cyl., cylinder; Tef., Teflon®; st, steel.

Fig. 13. Push test standard deviation versus publication year. Cyl., cylinder; Tef., Teflon®; st, steel.

Fig. 14. Scavuzzo and Chu 1987 data, strength versus temperature separated by temperature and ice thickness [48]. Outer marker color coded by thickness from blue-red, velocity by shape. Every third thickness denoted by fill. Marker size is approximately proportional to velocity. (a) Aluminum. (b) Steel. v, velocity in m/s; t, thickness in mm.

Fig. 15. Data from Druez et al. [78]. A, 0.4 g/m^3 liquid water content (LWC) and 20 µm mean volume diameter (MVD); B, 0.8 g/m^3 LWC and 40 µm MVD; v, velocity in m/s.

Fig. 16. Raraty and Tabor's rotational shearing apparatus [118]. (a) Cylindrical. (b) Annular.

Fig. 17. Adhesion strength versus time to peak load, calculated results from Oksanen [26] and measured results by Parameswaran [43], sourced from Oksanen [26]. Data not included elsewhere in this paper.

Fig. 18. (a) Stress distribution of 0° cone test (redrawn from Haehnel and Mulherin [110]). (b) Diagram of 0° cone test. LVDT, linear variable differential transformer.

Fig. 19. Makkonen's finite element analysis (FEA) results showing thermally induced stresses in the ice for a 0° cone test. (Reprinted with permission of VSP via Copyright Clearance Center from [9], ©2012 Journal of Adhesion Science & Technology by VSP.)

Fig. 20. Adhesion data from shear tests in the literature. Cyl., cylinder; poly., polyurethane; Tef., Teflon®.

Fig. 21. Standard deviation of shear tests in the literature. Cyl., cylinder; poly., polyurethane; Tef., Teflon®.

Fig. 22. Parametric studies data. (a) Adhesion strength versus average roughness on aluminum [120]. (b) Adhesion strength versus strain rate on steel [110]. Trend lines added.

Fig. 23. Raraty and Tabor's data [118]. Fit lines added, equations shown matching placement order on left side of trend line. Data not included in other figures since no repeats were performed.

Fig. 24. Tensile test blocks from 1939 [5].

Fig. 25. Simulation results for an ice sample on an aluminum substrate in tension, shear stress through thickness of ice. (a) 5 mm thick ice. (b) 2 mm thick ice). Dist., distance. (Reprinted with permission of Elsevier from [156], © 2011 Elsevier. DOI:10.1016/j.coldregions.2010.09.002)

Fig. 26. Stress analysis on vibrating composite ice-aluminum beam using Abaqus (Dassault Systems). (Reprinted with permission of IOP Publishing via Copyright Clearance Center from [152], © IOP Publishing. All rights reserved. DOI: 10.1088/0957-0233/21/7/075701)

Fig. 27. Replicated fracture surfaces. (a) Fine grained ice/steel interface. (b) Tap water ice/steel interface. (c) Single crystal of ice/steel interface. Arrows show crack propagation direction. (Reprinted with permission of Springer from [144], © Springer.)

Fig. 28. Sample blister test geometry. (a) Polytetrafluoroethylene (PTFE) thick "defect" disc (1 mm). (b) PTFE thin "defect" disc (50 μm). (c) Pressurized air supplied to release ice. (Reprinted with permission from [149], © Yong Yeong.)

Fig. 29. Roughness versus adhesion strength [152]. Bad data contained three extra values Yeong et al. excluded because of being erroneously high. Trend line added.

Fig. 30. Data from miscellaneous tests in the literature. Cantil., cantilevered; poly., polyurethane; spall., spallation; tens., tensioned; tors., torsioned; vib., vibrating.

Fig. 31. Standard deviation values from miscellaneous tests in the literature. Cantil., cantilevered; poly., polyurethane; spall., spallation; tens., tensioned; tors., torsioned; vib., vibration.

Fig. 32. Combined standard deviation data for aluminum versus number of repeats, grouped by test category (see previous figures for references). CAT, Centrifuge Adhesion Test.

Fig. 33. Combined standard deviation data for steel versus number of repeats, grouped by test category (see previous figures for references). CAT, Centrifuge Adhesion Test.

Fig. 34. Combined data for aluminum versus temperature, grouped by test category (see previous figures for references). CAT, Centrifuge Adhesion Test.

Fig. 35. Combined data for steel versus temperature, grouped by test category (see previous figures for references). CAT, Centrifuge Adhesion Test.

Fig. 36. Combined data for Teflon® and polyurethane versus temperature, grouped by publication. Poly, polyurethane; Tef. Teflon®; vib., vibrating.

Fig. 37. Combined data for aluminum versus velocity, grouped by test category (see previous figures for references). CAT, Centrifuge Adhesion Test.

Fig. 38. Combined data for steel versus velocity, grouped by test category (see previous figures for references). CAT, Centrifuge Adhesion Test.

5 References

1. Schoen JW. Tab for winter flight cancellations: $2.4 billion. CNBC. 2015. http://www.cnbc.com/2015/03/02/tab-for-winter-flight-cancellations-24-billion.html

2. Green SD. A study of U.S. inflight icing accidents and incidents, 1978 to 2002. In: 44th AIAA Aerospace Sciences Meeting and Exhibit. American Institute of Aeronautics and Astronautics. 2006.

3. Knight M, Clay WC. Refrigerated wind tunnel tests on surface coatings for preventing ice formation. NACA-TN-339. 1930.

4. Geer WC, Scott M. The prevention of the ice hazard on airplanes. NACA-TN-345. 1930.

5. Rothrick A, Selden R. Adhesion of ice in its relation to the de-icing of airplanes. NACA-TN-723. 1939.

6. Ford TF, Nichols OD. Adhesion-shear strength of ice frozen to clean and lubricated surfaces. NRL-5832. 1962.

7. Minsk DL. Ice adhesion tests on coatings subjected to rain erosion. CRREL-80-28. 1980.

8. Mulherin ND, Haehnel RB. Progress in evaluating surface coatings for icing control at corps hydraulic structures. Ice Engineering. ERDC/CRREL Technical Note 03-4. 2003.

9. Makkonen L. Ice adhesion—Theory, measurements and countermeasures. J Adhes Sci Technol 2012;26(4-5):413-445.

10. Merkle EL. Icing tunnel tests of icephobic coatings. In: Proceedings of the 8th National Conference on Environmental Effects of Aircraft and Propulsion Systems. Institute of Environmental Sciences. 1968. p. 25-31.

11. Phan, CL, McComber P, Mansiaux A. Adhesion of rime and glaze on conductors protected by various materials. Trans Can Soc Mech Eng 1977;4(4):204-208.

12. Janjua ZA, Turnbull B, Choy KL, Pandis C, Liu J, Hou X, Choi K-S. Performance and durability tests of smart icephobic coatings to reduce ice adhesion. Appl Surf Sci 2017;407:555-564.

13. Yang S, Xia Q, Zhu L, Xue J, Wang Q, Chen Q-M. Research on the icephobic properties of fluoropolymer-based materials. Appl Surf Sci 2011;257(11):4956-4962.

14. Liu, Q, Yang Y, Huang M, Zhou Y, Liu Y, Liang X. Durability of a lubricant-infused electrospray silicon rubber surface as an anti-icing coating. Appl Surf Sci 2015;346:68-76.

15. Wang S, Yang Z, Gong G, Wang J, Wu J, Yang S, Jiang L. Icephobicity of penguins spheniscus humboldti and an artificial replica of penguin feather with air-infused hierarchical rough structures. J Phys Chem C 2016;120:15923-15929.

16. Wang Y, Xi Y, Chen J, He Z, Liu J, Li Q, Wang J, Jiang L. Organogel as durable anti-icing coatings. SCM 2015;58(7):559-565.

17. Subramanyam SB, Rykaczewski K, Varanasi KK. Ice adhesion on lubricant-impregnated textured surfaces. Langmuir 2013;29(44):13414-13418.

18. Laforte C, Beisswenger A. Icephobic material centrifuge adhesion test. In: Proceedings of the 11th International Workshop on Atmospheric Icing of Structures. Montréal. 2005.

19. Meuler AJ, Smith JD, Varanasi KK, Mabry JM, McKinley GH, Cohen RE. Relationships between water wettability and ice adhesion. ACS Appl Mater Interfaces 2010;2(11):3100-3110.

20. Kreder MJ, Alvarenga J, Kim P, Aizenberg J. Design of anti-icing surfaces: smooth, textured or slippery? Nature Reviews Materials 2016;1:15003.

21. Sojoudi H, Wang M, Boscher ND, McKinley GH, Gleason, KK. Durable and scalable icephobic surfaces: similarities and distinctions from superhydrophobic surfaces. Soft Matter 2016;12(7):1938-1963.

22. Lv J, Song Y, Jiang L, Wang J, Bio-inspired strategies for anti-icing. ACS Nano 2014;8(4):3152-3169.

23. Kasaai MR, Farzaneh M. A critical review of evaluation methods of ice adhesion strength on the surface of materials. In: ASME 2004 23rd International Conference on Offshore Mechanics and Arctic Engineering. American Society of Mechanical Engineers. 2004.

24. Boluk Y, Adhesion of freezing precipitates to aircraft surfaces. Montreal Transportation Development Centre. 1996.

25. Schulz M, Sinapius M. Evaluation of different ice adhesion tests for mechanical deicing systems. SAE Technical Paper 2015-01-2135. 2015.

26. Oksanen P. Friction and adhesion of ice. Dissertation, Helsinki University of Technology. 1983.

27. Anderson DN, Reich AD. Tests of the performance of coatings for low ice adhesion. In: Prepared for the 35th Aerospace Sciences Meeting & Exhibit sponsored by the American Institute of Aeronautics and Astronautics. National Aeronautics and Space Administration. 1997.

28. Hobbs PV. Ice physics. Oxford: Clarendon Press. 1974.

29. Chu M, Scavuzzo R, Kellackey CJ. Tensile properties of impact ices. In: 30th Aerospace Sciences Meeting and Exhibit. American Institute of Aeronautics and Astronautics. 1992.

30. Reich AD, Scavuzzo RJ, and Chu ML. Survey of mechanical properties of impact ice. In: 32nd Aerospace Sciences Meeting and Exhibit. American Institute of Aeronautics and Astronautics. 1994.

31. Druez J, Claveau L, Tremblay C. La mesure de la résistance en traction de la glace atmosphérique. Comptes rendus du onzième Congrès Canadien de Mécanique Appliquée, Université d'Alberta, Edmonton, 1987. p. 236-237.

32. Steen LE, Ide RF, Van Zante JF. An assessment of the SEA multi-element sensor for liquid water content calibration of the NASA GRC Icing Research Tunnel. In: SAE 2015 International Conference on Icing of Aircraft, Engines, and Structures. SAE International. 2015.

33. Steen, LE, Ide RF, Van Zante JF, Acosta WJ. NASA Glenn Icing Research Tunnel: 2014 and 2015 cloud calibration procedures and results. NASA/TM—2015-218758. 2015.

34. Stallabrass, JR, Price RD. On the adhesion of ice to various materials. Aeronautical Report LR-350. National Research Council Canada. 1962.

35. Beams JW, Breazeale JB, Bart W. Mechanical strength of thin films of metals. Phys Rev 1955;100(6):1657-1661.

36. Itagaki K. Mechanical ice release processes. Part 1: Self-shedding of accreted ice from high speed rotors. CRREL-83-26. US Army Cold Regions Research and Engineering Laboratory. 1983.

37. Plump R. Ice adhesion studies. Technical Note, Internal Data Report. US Army Cold Regions Research and Engineering Laboratory. 1968.

38. Loughborough D. The physics of the mechanical removal of ice from aircraft. Aeronautical Engineering Review, 1952;11(2):29-34.

39. Yoshida M, et al. Adhesion of ice to various materials. In: Cold Regions Technology Conference. 1991.

40. Aubert R. History of ice protection system design at Bell Helicopter. SAE Technical Paper 2003-01-2093. 2003.

41. Jones JR, Gardos MN. Adhesive shear strength of ice to bonded solid lubricants. Lubr Eng 1972; 28(12):464-471.

42. Chu ML. Measurement of adhesive shear strength of impact ice in an icing wind tunnel. In: Proceedings of the Third International Workshop on the Atmospheric Icing of Structures, Environment Canada. 1991.

43. Parameswaran VR. Adfreeze strength of model piles in ice. Can Geotech J 1981;18(1):8-16.

44. Fortin G. Considerations on the use of hydrophobic, superhydrophobic or icephobic coatings as a part of the aircraft ice protection system. SAE Technical Paper 2013-01-2108. 2013.

45. Rohatgi A. WebPlotDigitizer. PLOTCON 2017. 2017.

46. Tarquini S, Antonini C, Amirfazli A, Marengo M, Palacios J. Investigation of ice shedding properties of superhydrophobic coatings on helicopter blades. Cold Reg Sci Technol 2014;100:50-58.

47. Soltis J, Palacios J, Eden T, Wolfe D. Evaluation of ice-adhesion strength on erosion-resistant materials. AIAA J 2014;53(7):1825-1835.

48. Scavuzzo RJ, Chu ML. Structural properties of impact ices accreted on aircraft structures. NASA Contractor Report 179580. 1987.

49. Chu M, Scavuzzo RJ. Adhesive shear strength of impact ice. AIAA J 1991;29(11):1921-1926.

50. Loughborough DL, Haas EG. Reduction of the adhesion of ice to de-icer surfaces. J Aeronaut Sci 1946;13(3):126-134.

51. Itagaki K. Mechanical ice release processes. I. Self-shedding from high-speed rotors. CRREL-83-26. 1983.

52. Beisswenger A, Fortin G, Laforte C. Advances in ice adherence and accumulation reduction testing at the Anti-Icing Materials International Laboratory (AMIL). Future De-Icing Technologies, Berlin. 2010.

53. Laforte C, Blackburn C, Perron J. A review of icephobic coating performances over the last decade. SAE Technical Paper 2015-01-2149. 2015.

54. Menini R, Farzaneh M. Elaboration of Al_2O_3/PTFE icephobic coatings for protecting aluminum surfaces. Surf Coat Technol 2009;203(14):1941-1946.

55. Menini R, Ghalmi Z, Farzaneh M. Highly resistant icephobic coatings on aluminum alloys. Cold Reg Sci Technol 2011;65(1):65-69.

56. Farhadi S, Farzaneh M, Kulinich S. Anti-icing performance of superhydrophobic surfaces. Appl Surf Sci 2011;257(14):6264-6269.

57. Kulinich S, Farhadi S, Nose K, Dull XW. Superhydrophobic surfaces: Are they really ice-repellent? Langmuir. 2011;27(1):25-29.

58. Kulinich S, Farzaneh M. Ice adhesion on super-hydrophobic surfaces. Appl Surf Sci 2009; 255(18):8153-8157.

59. Kulinich SA, Farzaneh M. How wetting hysteresis influences ice adhesion strength on superhydrophobic surfaces. Langmuir 2009;25(16):8854-8856.

60. Kulinich S, Farzaneh M. On ice-releasing properties of rough hydrophobic coatings. Cold Reg Sci Technol 2011;65(1):60-64.

61. Fortin G, Adomou M, Perron J. Experimental study of hybrid anti-icing systems combining thermoelectric and hydrophobic coatings. SAE Technical Paper 2011-38-0003. 2011.

62. Fortin G, Perron J. Spinning rotor blade tests in icing wind tunnel. In: 1st AIAA Atmospheric and Space Environments Conference. AIAA 2009-4260. 2009.

63. Brouwers E, Palacios J, Peterson A, Centolanza L. Ice adhesion strength measurements for rotor blade leading edge materials. Presented at the American Helicopter Society 67th Annual Forum. American Helicopter Society International, Inc. 2011.

64. Palacios J, Wolfe D, Bailey M, Szefi J. Ice testing of a centrifugally powered pneumatic deicing system for helicopter rotor blades. JAHS 2015;60(3):1-12.

65. Soltis J, Palacios J, Eden T, Wolfe D. Ice adhesion mechanisms of erosion-resistant coatings. AIAA J 2014;53(3):654-662.

66. Smith J, Wohl CJ, Kreeger RE, Palacios J, Knuth T, Hadley K. Effect of molecular flexibility upon ice adhesion shear strength. In: 39th Annual Meeting of the Adhesion Society. Adhesion Society, Inc. 2016.

67. Stenroos C, Koivuluoto H, Bolelli G, Ruohomaa R, Lusvarghi L, Vuoristo P. Research on icing behavior and ice adhesion testing of icephobic surfaces. In: 16th International Workshop on Atmospheric Icing of Structures. 2015:6.

68. Chanda J, Ionov L, Kirillova A, Synytska A. New insight into icing and de-icing properties of hydrophobic and hydrophilic structured surfaces based on core–shell particles. Soft Matter 2015;11(47):9126-9134.

69. Saleema N, Farzaneh M, Paynter RW, Sarkar DK. Prevention of ice accretion on aluminum surfaces by enhancing their hydrophobic properties. J Adhes Sci Technol 2011;25(1-3):27-40.

70. Fortin G, Beisswenger A, Perron J. Centrifuge adhesion tests to evaluate icephobic coatings. In: AIAA Atmospheric and Space Environments Conference. AIAA 2010-7837. 2010.

71. Dotan A, Dodiuk H, Laforte C, Kenig S. The relationship between water wetting and ice adhesion. J Adhes Sci Technol 2009;23(15):1907-1915.

72. Freiberger A, Lacks H, Quatinetz M. Method and apparatus for selection and comparison of the adhesion of ice to surfaces and coatings. U.S. Patent 3030797 A. 1962.

73. Lacks H, Quatinetz M, Freiberger A. Ice adhesion apparatus and test method. ASTM Bull 1957;224:48-50.

74. Landy M, Freiberger A. Studies of ice adhesion: I. Adhesion of ice to plastics. J Colloid Interface Sci 1967;25(2):231-244.

75. Baker HR, Bascom WD, Singleterry CR. The adhesion of ice to lubricated surfaces. J Colloid Sci 1962;17(5):477-491.

76. Bascom WD, Cottington RL, Singleterry CR. Ice adhesion to hydrophilic and hydrophobic surfaces. J Adhes 1969;1(4):246-263.

77. Jellinek HHG, Kachi H, Kittaka S, Lee M, Yokota R. Ice releasing block-copolymer coatings. Colloid Polym Sci 1978;256(6):544-551.

78. Druez J, Nguyen D, Lavoie Y. Mechanical properties of atmospheric ice. Cold Reg Sci Technol 1986;13(1):67-74.

79. Druez J, Phan CL, Laforte JL, Nguyen DD. The adhesion of glaze and rime on aluminum electrical conductors. Trans Can Soc Mech Eng 1979;5(4):215-220.

80. Chen J, et al. Robust prototypical anti-icing coatings with a self-lubricating liquid water layer between ice and substrate. ACS Appl Mater Interfaces 2013;5(10):4026-4030.

81. Chen J, et al. Superhydrophobic surfaces cannot reduce ice adhesion. Appl Phys Lett 2012;101(11): 111603.

82. Chernyy S, et al. Superhydrophilic: Polyelectrolyte brush layers with imparted anti-icing properties: Effect of counter ions. ACS Appl Mater Interfaces 2014;6(9):6487-6496.

83. Dou R, Chen J, Zhang Y, Wang X, Cui D, Song Y, Jiang L, Wang J. Anti-icing coating with an aqueous lubricating layer. ACS Appl Mater Interfaces 2014;6(10):6998-7003.

84. Fu Q, et al. Development of sol–gel icephobic coatings: Effect of surface roughness and surface energy. ACS Appl Mater Interfaces 2014;6(23):20685-20692.

85. Ge L, Guifu D, Hong W, Yao J, Cheng P, Wang Y. Anti-icing property of superhydrophobic octadecyltrichlorosilane film and its ice adhesion strength. J Nanomater 2013;2013:278936.

86. Golovin K, Kobaku SP, Lee DH, DiLoreto ET, Mabry JM, Tuteja A. Designing durable icephobic surfaces. Sci Adv 2016;2(3):e1501496.

87. He Z, Vagenes ET, Delabahan C, He J, Zhang Z. Room temperature characteristics of polymer-based low ice adhesion surfaces. Sci Rep 2017;7:42181.

88. Hejazi V, Sobolev K, Nosonovsky M. From superhydrophobicity to icephobicity: Forces and interaction analysis. Sci Rep 2013;3:2194.

89. Kim JW. Development of a physics based methodology for the prediction of rotor blade ice formation. Dissertation, Georgia Institute of Technology. 2015.

90. Kim P, Wong T-K, Alvarenga J, Kreder MJ, Adorno-Martinez WE, Aizenber J. Liquid-infused nanostructured surfaces with extreme anti-ice and anti-frost performance. ACS Nano 2012;6(8):6569-6577.

91. Kraj AG, Bibeau EL. Measurement method and results of ice adhesion force on the curved surface of a wind turbine blade. Renewable Ener 2010;35(4):741-746.

92. Lou D, Hammond D, Pervier M-L. Investigation of the adhesive properties of the ice–aluminum interface. J Aircr 2014;51(3):1051-1056.

93. Lynch D, Ludwiczak DR. Shear strength analysis of the aluminum/ice adhesive bond. NASA TM-107162. 1996.

94. Murase H, Nanishi K. On the relationship of thermodynamic and physical properties of polymers with ice adhesion. Ann Glaciol 1985;6(1):146-149.

95. Saito H, Takai K, Yamauchi G. Water-and ice-repellent coatings. Surf Coat Int B: Coat Trans 1997;80(4):168-171.

96. Smith JD, Meuler AJ, Bralower HL, Venkatesan R, Subramanian S, Cohen RE, McKinley GH, Varanasi KK. Hydrate-phobic surfaces: Fundamental studies in clathrate hydrate adhesion reduction. Phys Chem Chem Phys 2012;14:6013-6020.

97. Sojoudi H, McKinley GH, Gleason KK. Linker-free grafting of fluorinated polymeric cross-linked network bilayers for durable reduction of ice adhesion. Mater Horiz 2015;2:91-99.

98. Varanasi KK, Deng T, Smith JD, Hsu M, Bhate N. Frost formation and ice adhesion on superhydrophobic surfaces. Appl Phys Lett 2010;97(23):234102.

99. Venkataramani K. Experimental study of ice adhesion on aircraft engine airfoils. In: 41st Aerospace Sciences Meeting and Exhibit. AIAA 2003-732. 2003.

100. Vogel N, Belisle RA, Hatton B, Wong T-S, Aizenberg J. Transparency and damage tolerance of patternable omniphobic lubricated surfaces based on inverse colloidal monolayers. Nat Commun 2013;4:2176.

101. Wang Y, Xue J, Wang Q, Chen Q, Ding J. Verification of icephobic/anti-icing properties of a superhydrophobic surface. ACS Appl Mater Interfaces 2013;5(8):3370-3381.

102. Wang C, Fuller T, Zhang W, Wynne KJ. Thickness dependence of ice removal stress for a polydimethylsiloxane nanocomposite: Sylgard 184. Langmuir 2014;30(43):12819-12826.

103. Zou M, Beckford S, Wei R, Ellis C, Hatton G, Miller MA. Effects of surface roughness and energy on ice adhesion strength. Appl Surf Sci 2011;257(8):3786-3792.

104. Wang C, Zhang W, Siva A, Tiea D, Wynne KJ. Laboratory test for ice adhesion strength using commercial instrumentation. Langmuir 2013;30(2):540-547.

105. Alansatan S, Papadakis M. Experimental investigation of ice adhesion. SAE Technical Paper 1999-01-1584. 1999.

106. Andersson L-O, Golander C-G, Persson S. Ice adhesion to rubber materials. J Adhes Sci Technol 1994;8(2):117-132.

107. Bharathidasan T, Kimar SV, Bobji MS, Chakradhar RPS, Basu BJ. Effect of wettability and surface roughness on ice-adhesion strength of hydrophilic, hydrophobic and superhydrophobic surfaces. Appl Surf Sci 2014;314:241-250.

108. Croutch VK, Hartley RA, Adhesion of ice to coatings and the performance of ice release coatings. J Coat Technol 1992;64(815):41-53.

109. Gouni R. A new technique to study temperature effects on ice adhesion strength for wind turbine materials. Master of Science Thesis, Case Western Reserve University. 2011.

110. Haehnel R, Mulherin N. The bond strength of an ice–solid interface loaded in shear. In: Shen HT, editor. Ice in Surface Waters. Proceedings of the 14th International Symposium on Ice. Kinokuniya Company Ltd. 1998.

111. Jellinek H. Ice adhesion. Can J Phys 1962;40(10):1294-1309.

112. Jellinek H. Adhesive properties of ice: Part II. U.S. Army Snow Ice and Permafrost Research Establishment. Research Report 62. Corps of Engineers. 1960.

113. Mulherin ND, Richter-Menge JA, Tantillo TJ, Gould LD, Durell GD, Elder BC. Laboratory test for measurement of adhesion strength of spray ice to coated flat plates. CRREL Report 560 90-2. 1990.

114. Palacios J, Smith E, Rose J, Royer R. Instantaneous de-icing of freezer ice via ultrasonic actuation. AIAA J 2011;49(6):1158-1167.

115. Petrenko V, Courville Z. Active de-icing coating for aerofoils. In: 38th Aerospace Sciences Meeting and Exhibit. American Institute of Aeronautics and Astronautics. 2000.

116. Petrenko VF, Peng S. Reduction of ice adhesion to metal by using self-assembling monolayers (SAMs). Can J Phys 2003;81(1-2):387-393.

117. Petrenko VF, Qi S. Reduction of ice adhesion to stainless steel by ice electrolysis. J Appl Phys 1999; 86:5450-5454.

118. Raraty LE, Tabor D. The adhesion and strength properties of ice. Proc R Soc A 1958;245(1241): 184-201.

119. Saeki H, Ono T, Zong NE, Nakazawa N. Experimental study on direct shear strength of sea ice. Ann Glaciol 1985;6(1):218-221.

120. Susoff M, Siegmann K, Pfaffenroth C, Hirayama M. Evaluation of icephobic coatings—Screening of different coatings and influence of roughness. Appl Surf Sci 2013;282:870-879.

121. Terashima T. Comparative experiments on various adfreeze bond strength tests between ice and materials. WIT Trans Eng Sci 1997;14:205-215.

122. Zhu L, Xue J, Wang Y, Chen Q, Ding J, Wang Q. Ice-phobic coatings based on silicon-oil-infused polydimethylsiloxane. ACS Appl Mater Interfaces 2013;5(10):4053-4062.

123. Scavuzzo RJ, Chu ML, Kellackey CJ. Impact ice stresses in rotating airfoils. J Aircr 1991;28(7):450-455.

124. Yeong YH, Milionis A, Loth E. Atmospheric ice adhesion on water-repellent coatings: Wetting and surface topology effects. Langmuir 2015;31(48):13107-13116.

125. Jellinek HHG, Brill R, Viscoelastic properties of ice. J Appl Phys 1956;27(10):1198-1209.

126. Jellinek HHG. Tensile strength properties of ice adhering to stainless steel. Snow Ice and Permafrost Research Establishment. 1957.

127. Jellinek HHG. The influence of imperfections on the strength of ice. Proc Phys Soc 1958;71(5):797.

128. Jellinek HHG. Liquid-like (transition) layer on ice. Adv Colloid Interface Sci 1967;25(2):192-205.

129. Reich A. Interface influences upon ice adhesion to airfoil materials. AIAA 32nd Aerospace Sciences Meeting and Exhibit. AIAA 94-0714. 1994.

130. Magnum Engineers. Ice adhesion test rig TE-10K-IAT. 2017. http://magnumengg.com/product/ice-adhesion-test-rig-te-10k-iat/

131. Office of the Chief of Engineers. Engineering and design. Ice engineering. Engineer Manual EM 1110-2-1612. 2006.

132. Ford TF, Nichols OD. Shear characteristics of ice in bulk, at ice/solid interfaces, and at ice/lubricant/solid interfaces, and at ice/lubricant/solid interfaces in a laboratory device. US Naval Research Laboratory Report NRL-5662. 1961.

133. Ojalvo IU, Eidinoff HL. Bond thickness effects upon stresses in single-lap adhesive joints. AIAA J 1978;16(3):204-211.

134. Makkonen L. Surface melting of ice. J Phys Chem B, 1997;101(32):6196-6200.

135. Bartels-Rausch T, et al. A review of air–ice chemical and physical interactions (AICI): liquids, quasi-liquids, and solids in snow. Atmos Chem Phys 2014;14(3):1587-1633.

136. Blackburn C, Laforte C, Laforte JL. Apparatus for measuring the adhesion force of a thin ice sheet on a substrate. Presented at the Ninth International Workshop on Atmospheric Icing of Structures. Anti-Icing Materials International Laboratory and University of Quebec at Chicoutimi. 2000.

137. Laforte C, Laforte JL, Carriere JC. How a solid coating can reduce the adhesion of ice on a structure. Presented at the Tenth International Workshop on Atmospheric Icing of Structures. 2002.

138. Laforte C, Laforte JL. Tensile, torsional and bending strain at the adhesive rupture of an iced substrate. In: Proceedings of the 28th International Conference on Ocean, Offshore and Arctic Engineering. American Society of Mechanical Engineers. 2009.

139. Hassan MF, Lee HP, Lim SP. The variation of ice adhesion strength with substrate surface roughness. Meas Sci Tech 2010;21(7):075701.

140. Strobl T, Raps D, Hornung M. Comparative evaluation of ice adhesion behavior. Int J Mech Aerosp Ind Mechatron Manuf Eng 2012;68(2012):68.

141. Javan-Mashmool M, Volat C, Farzaneh M. A new method for measuring ice adhesion strength at an ice—substrate interface. Hydrol Process 2006;20(4):645-655.

142. Akitegetse C, Volat C, Farzaneh M, Measuring bending stress on an ice/aluminium composite beam interface using an embedded piezoelectric PVDF (polyvinylidene-fluoride) film sensor. Meas Sci Technol 2008;19(6):065703.

143. Sarkar DK, Farzaneh M. Superhydrophobic coatings with reduced ice adhesion. J Adhes Sci Technol 2009;23(9):1215-1237.

144. Ruan M, Li W, Wang B, Deng B, Ma F, Yu Z. Preparation and anti-icing behavior of superhydrophobic surfaces on aluminum alloy substrates. Langmuir 2013;29(27):8482-8491.

145. Grimmer P, Ganesan S, Haupt M, Barz J. Energy efficient de-icing by superhydrophobic and icephobic polyurethane films created by microstructuring and plasma-coating. SAE Technical Paper 2015-01-2159. 2015.

146. Lee T-Y. The efect of impurities in water from Lake Erie on the adhesive strength of ice to wind turbine materials. Master of Science Thesis, Case Western Reserve University. 2011.

147. Cole DM. ERDC/CRREL nominal mode I ice adhesion testing. US Engineer Research and Development Center, Cold Regions Research and Engineering Laboratory. 2014.

148. Jiang KR, Penn LS. Use of the blister test to study the adhesion of brittle materials. Part II. Application. J Adhes 1990;32(4):217-226.

149. Jiang KR, Penn LS. Use of the blister test to study the adhesion of brittle materials. Part I. Test modification and validation. J Adhes 1990;32(4):203-216.

150. Andrews E, Lockington N. The cohesive and adhesive strength of ice. J Mater Sci 1983;18(5):1455-1465.

151. Davis A, Yeong YH, Steele A, Bayer IS, Loth E, Superhydrophobic nanocomposite surface topography and ice adhesion. ACS Appl Mater Interfaces 2014;6(12):9272-9279.

152. Yeong Y, Loth E, Sokhey J, Lambourne A. Ice adhesion strength on hydrophobic and superhydrophobic coatings. In: Proceedings of the 6th AIAA Atmospheric and Space Environments Conference. American Institute of Aeronautics and Astronautics. 2014.

153. Andrews E, Majid H, Lockington N. Adhesion of ice to a flexible substrate. J Mater Sci 1984; 19(1):73-81.

154. Archer P, Gupta V. Measurement and control of ice adhesion to aluminum 6061 alloy. J Mech Phys Solids 1998;46(10):1745-1771.

155. Wei Y, Adamson RM, Dempsey JP. Ice/metal interfaces: fracture energy and fractography. J Mater Sci 1996;31(4):943-947.

156. Riahi MM, Marceau D, Laforte C, Perron J. The experimental/numerical study to predict mechanical behaviour at the ice/aluminium interface. Cold Reg Sci Technol 2011;65(2):191-202.

157. Williams ML. The continuum interpretation for fracture and adhesion. J Appl Polym Sci 1969; 13(1):29-40.

158. Chen Y, Wenhao W, Dong W, Li M, Lie L. Numerical study on the adhesion strength between ice and aluminium based on a cohesive zone model. In: ASME Turbo Expo 2014: Turbine Technical Conference and Exposition. ASME GT2014-25171. 2014.

159. Fortin G, Perron J, Ice adhesion models to predict shear stress at shedding. J Adhes Sci Technol 2012;26(4-5):523-553.

160. Reinmann JJ, Shaw RJ, and Olsen Jr., WA. Aircraft icing research at NASA. NASA TM-82919. 1982.

Table 1. Standard deviation data for shear tests

Method	Aluminum (%)	Steel (%)	Polyurethane (%)	Teflon® (%)
Lap shear	27.5	31.7	27.9	156.1
0° cone	9.2	16.9		96.3
All methods	11.8	22.2	27.9	136.1

Table 2. Standard deviation data for miscellaneous tests[a]

Method	Aluminum (%)	Steel (%)	Polyurethane (%)
Tension	24.1	18.7	19.1
Torsioned Beam	76.3 (27.5*)		
Tensioned Beam	21.6		
Vibrating Beam	22.2		34.0
Laser Spallation	4.9		

[a]Excluding possibly erroneous values.

Table 3. Comparison of methods reviewed

Test method	Advantages	Disadvantages	Average scatter, %
CAT[b]	Throughput	SRC[c], sample variability, SP[d], edge effects, vibration	Al: 14.7 St:
CCAT[e]	Can obtain tensile and adhesion strength, in situ	SRC, uncommon, sample variability, vibration, edge effects, nonuniform load, SP	Al: 30.8 St:
ICAT[f]	Stress recorded, in situ	High sample variability, SRC, vibration, edge effects, SP	Al: St: 14.5
Push—nonimpact ice (with mold)	Throughput, repeatable geometry, SRC, SP, low noise	In situ impossible, aerodynamics	Al: 18.7 St: 10.8
Push—impact ice (without mold)	Throughput, in situ possible, SRC, SP, low noise	Sample variability, contact variability, aerodynamics	Al: 26.4 St: 15.9
Rotational Shear	Low-stress concentration, SRC, SP, low noise	Difficult geometry, not in situ	Al: St:
0° cone and similar	Well-understood stress distribution, SRC, SP, low noise	Thermal expansion, not in situ	Al: 9.2 St: 16.9
Lap shear	Low-stress concentration, SRC, SP, low noise, flexible methodology	Not in situ, edge effects for impact ice	Al: 27.5[a] St: 31.7
Tension	Mode 1, SRC, SP, low noise	Not in situ, edge effects for impact ice	Al: 24.1[a] St: 18.7
Beam tests (all)	SRC, simple geometry, flexible test method, SP, in situ possible for some	Substrate stiffness limiting, edge effects for impact ice	Al: 33.9 St:
Blister	Mode 1, low-cost equipment, simple geometry, SP, in situ	SRC, no stress-strain curve, edge effects for impact ice	Al: St:
Laser spallation	Mode 1, simple geometry, SP, in situ possible	Uncommon, erroneously high results, requires visual inspection (no rime ice)	Al: 4.9 St:
Peel	In situ, mode 1, SP	Complex structure, extremely uncommon, SRC	Al: St:

[a]Only one data point.

[b]Centrifuge Adhesion Test.

[c]Strain rate control.

[d]Sample preserving.

[e]Calculated CAT.

[f]Instrumented CAT.

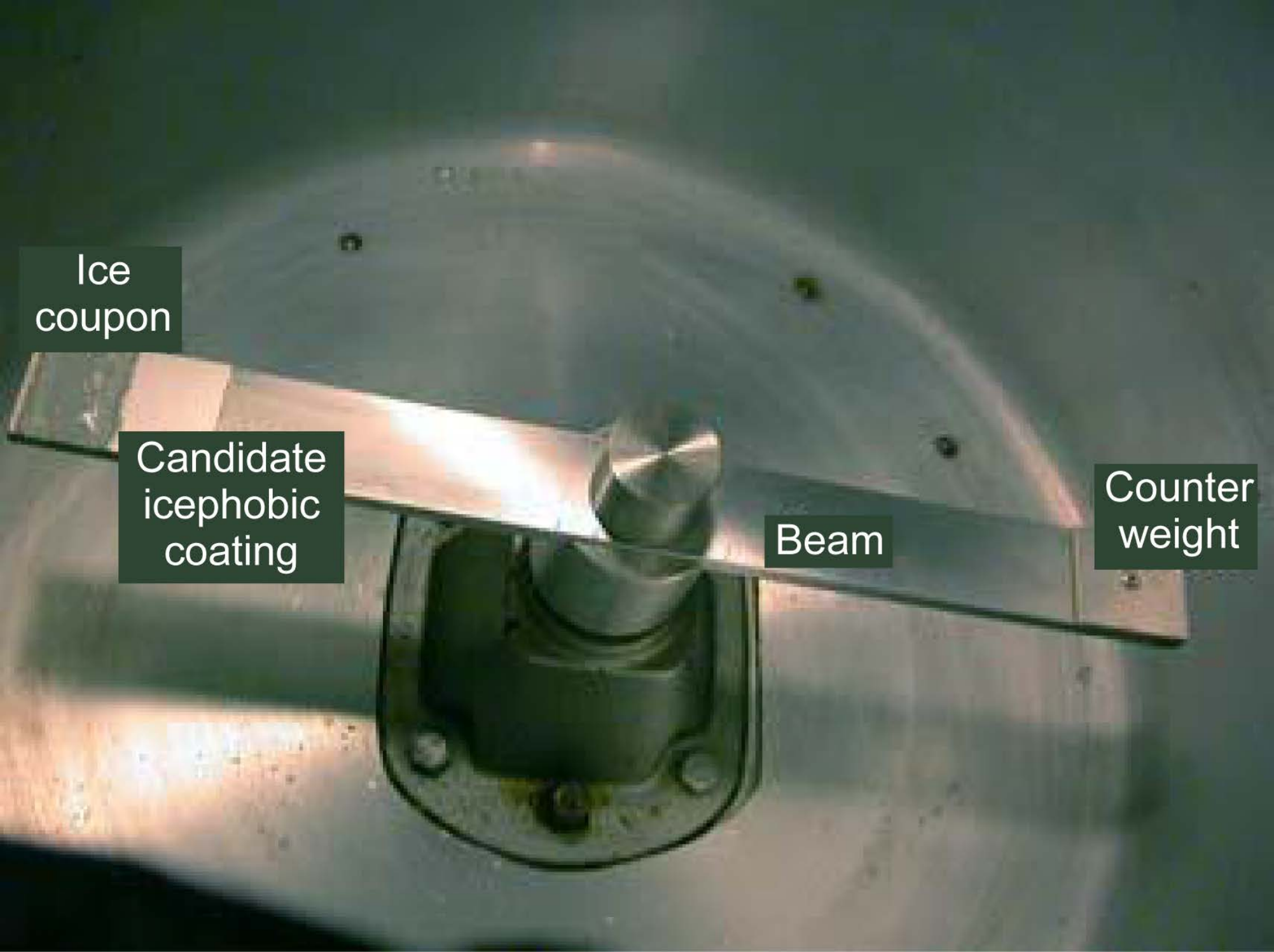
Ice coupon
Candidate icephobic coating
Beam
Counter weight

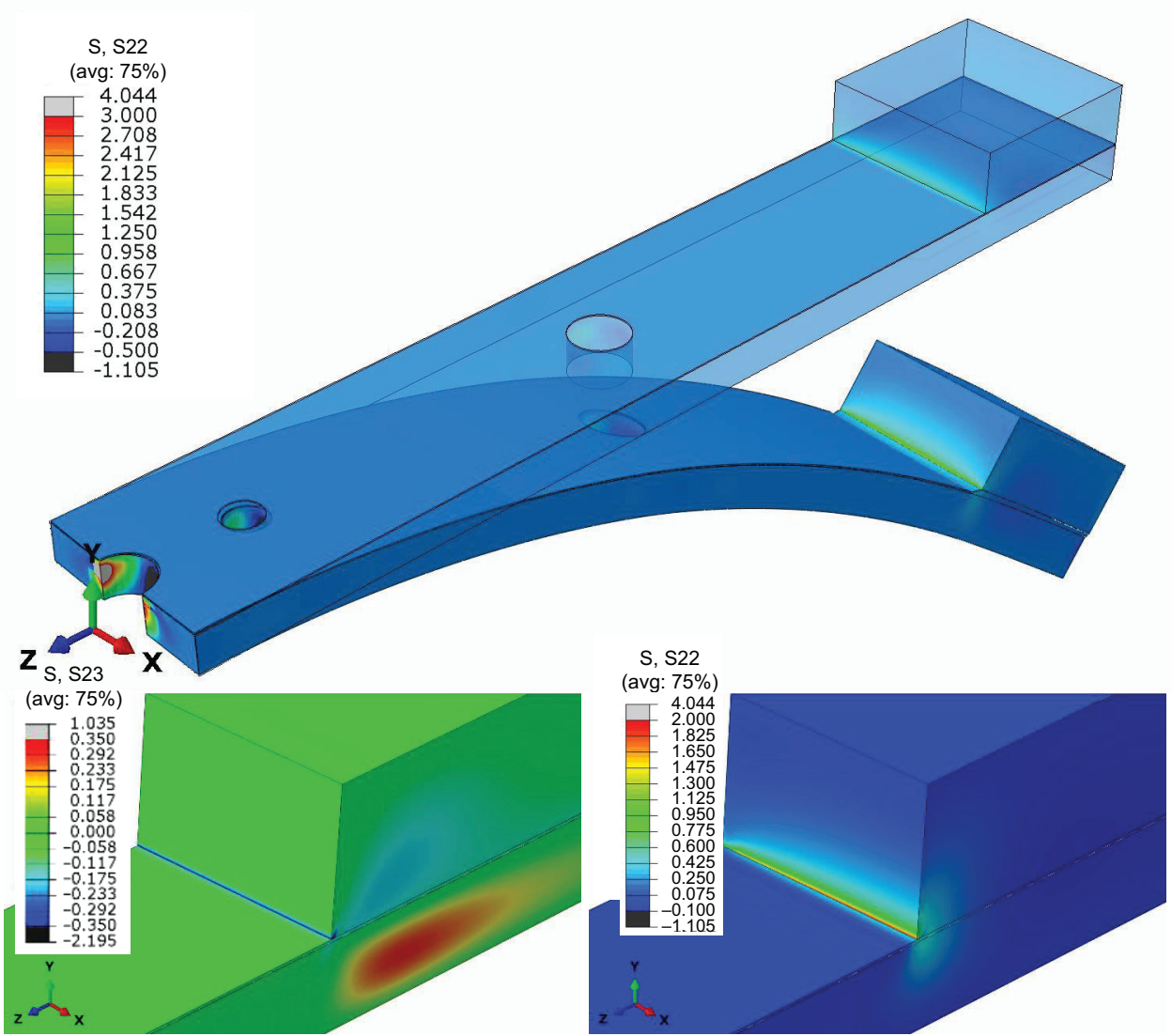
S, S22
(avg: 75%)
4.044
3.000
2.708
2.417
2.125
1.833
1.542
1.250
0.958
0.667
0.375
0.083
-0.208
-0.500
-1.105
Y
Z
X
S, S23
(avg: 75%)
1.035
0.350
0.292
0.233
0.175
0.117
0.058
0.000
-0.058
-0.117
-0.175
-0.233
-0.292
-0.350
-2.195
Y
Z
X
S, S22
(avg: 75%)
4.044
2.000
1.825
1.650
1.475
1.300
1.125
0.950
0.775
0.600
0.425
0.250
0.075
−0.100
−1.105
Y
Z
X

Figure 2

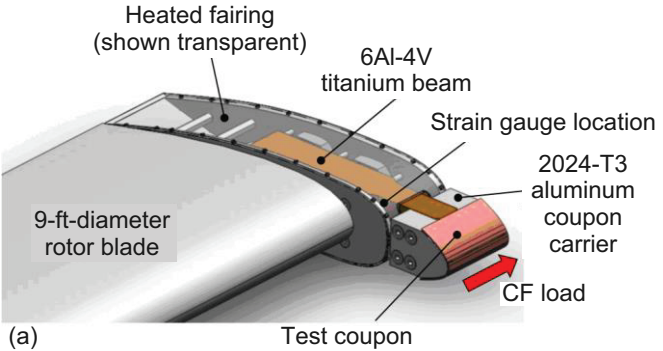
Heated fairing
(shown transparent)
6Al-4V
titanium beam
Strain gauge location
2024-T3
aluminum
coupon
carrier
9-ft-diameter
rotor blade
CF load
(a)
Test coupon

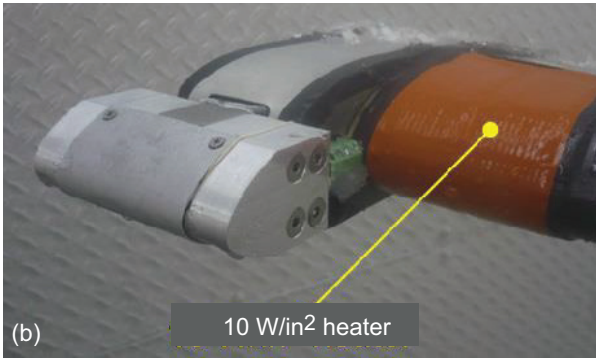
(b)
10 W/in2 heater

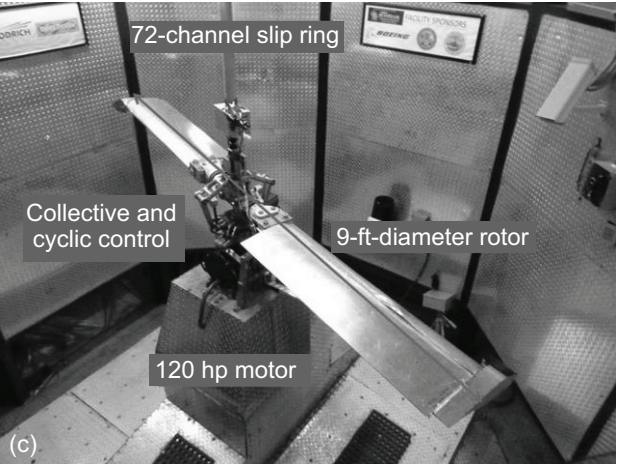
72-channel slip ring
Collective and
cyclic control
9-ft-diameter rotor
120 hp motor
(c)

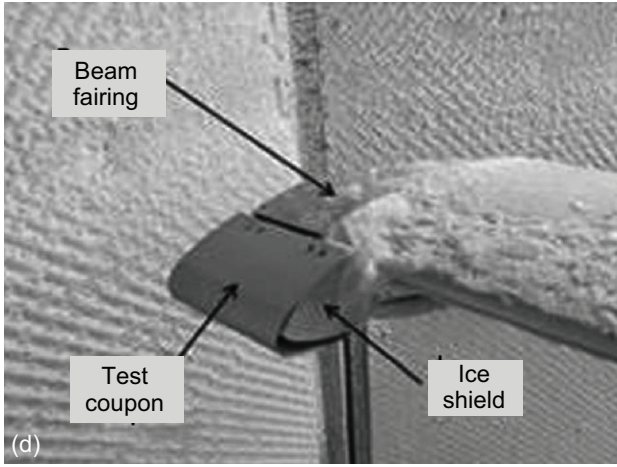
Beam
fairing
Test
coupon
Ice
shield
(d)

Figure 3

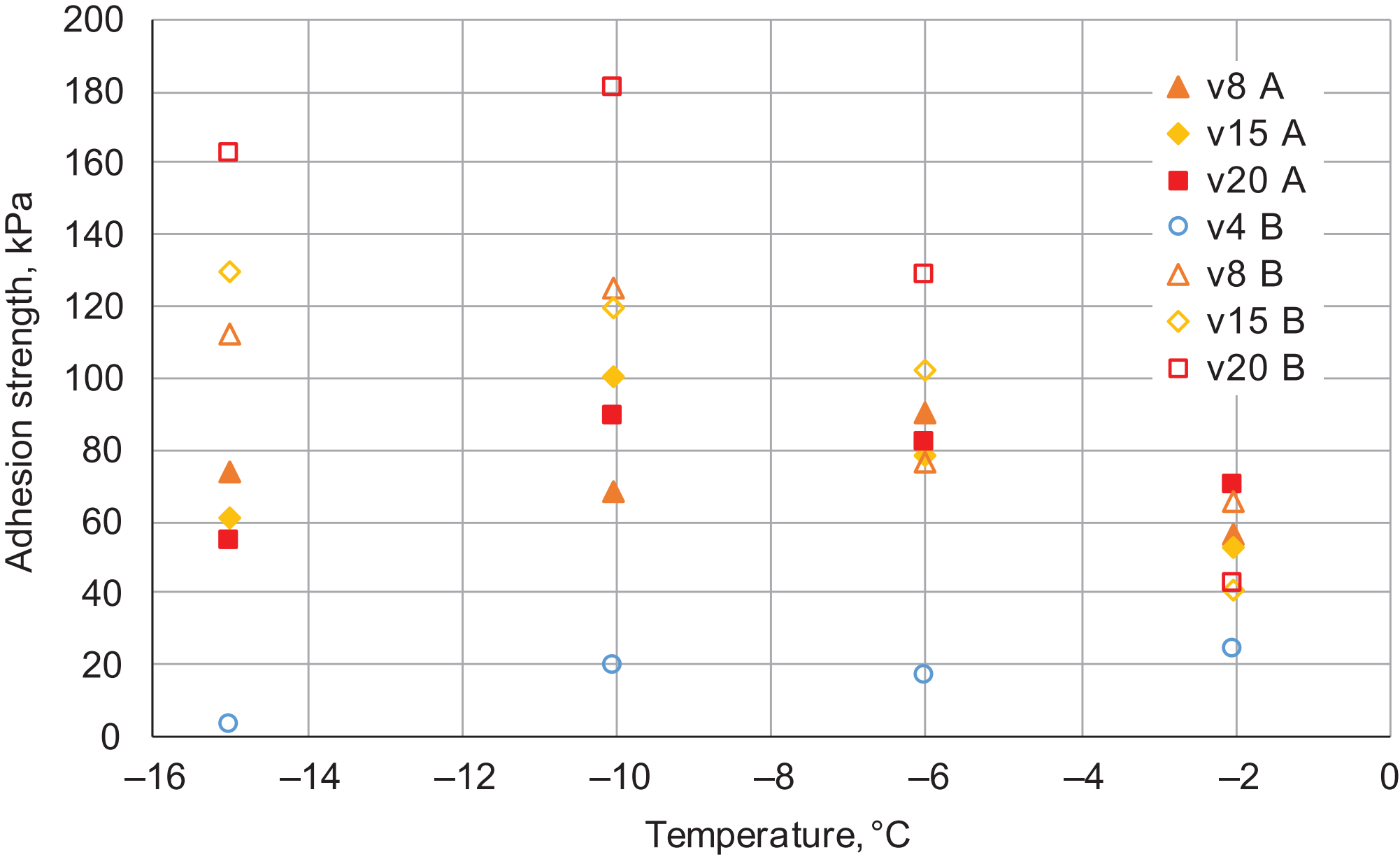
Adhesion strength, kPa
200
180
160
140
120
100
80
60
40
20
0
–16
–14
–12
–10
–8
–6
–4
–2
0
Temperature, °C
v8 A
v15 A
v20 A
v4 B
v8 B
v15 B
v20 B

Figure 15

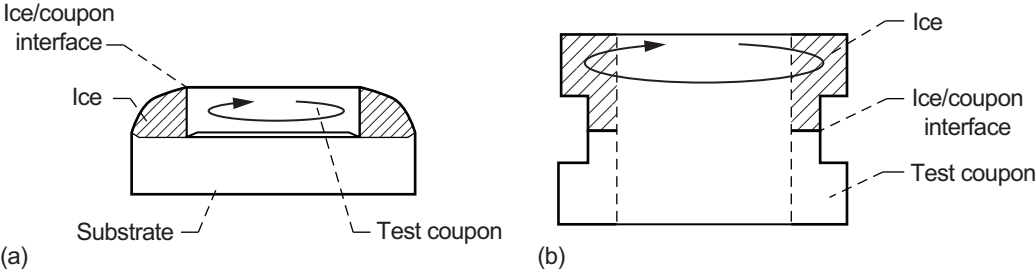
Ice/coupon
interface
Ice
Substrate
Test coupon
(a)
Ice
Ice/coupon
interface
Test coupon
(b)

Figure 16

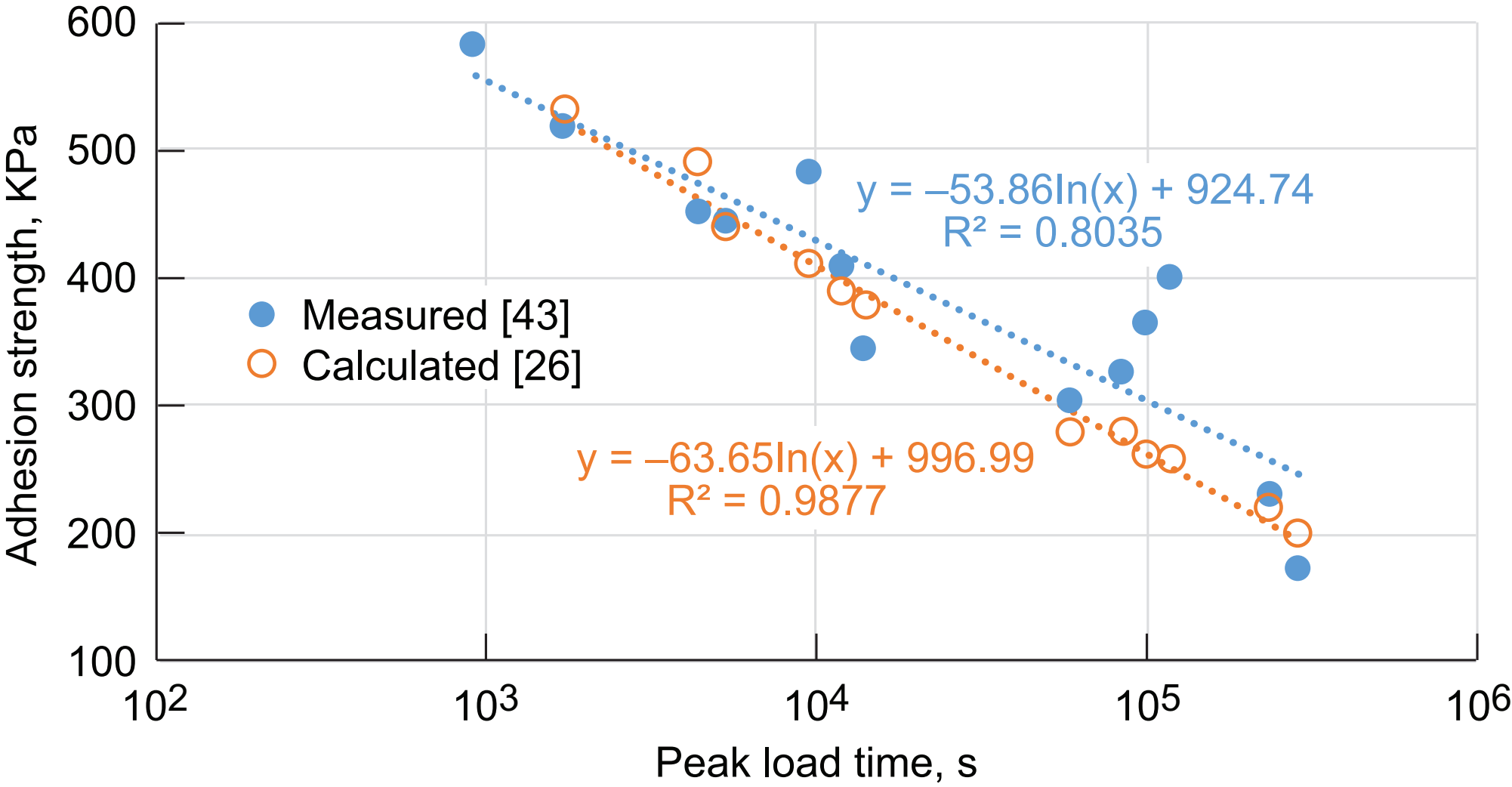
600
500
400
300
200
100
Adhesion strength, KPa
Measured [43]
Calculated [26]
y = –53.86ln(x) + 924.74
R² = 0.8035
y = –63.65ln(x) + 996.99
R² = 0.9877
10²
10³
10⁴
10⁵
10⁶
Peak load time, s

Figure 17

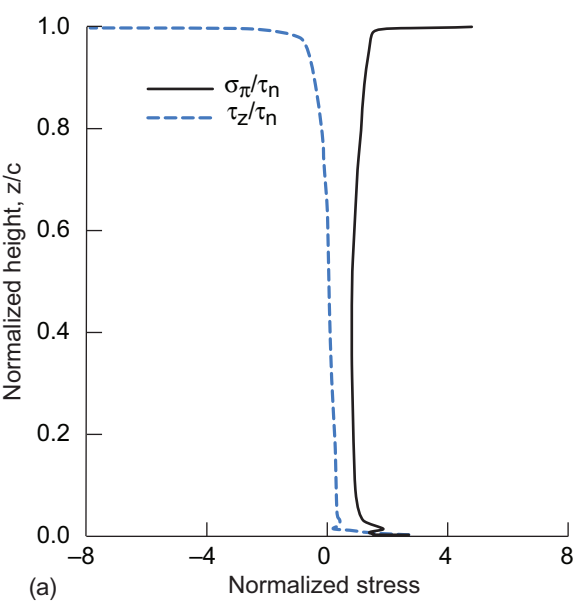
1.0
0.8
0.6
0.4
0.2
0.0
Normalized height, z/c
σπ/τn
τz/τn
–8
–4
0
4
8
Normalized stress
(a)

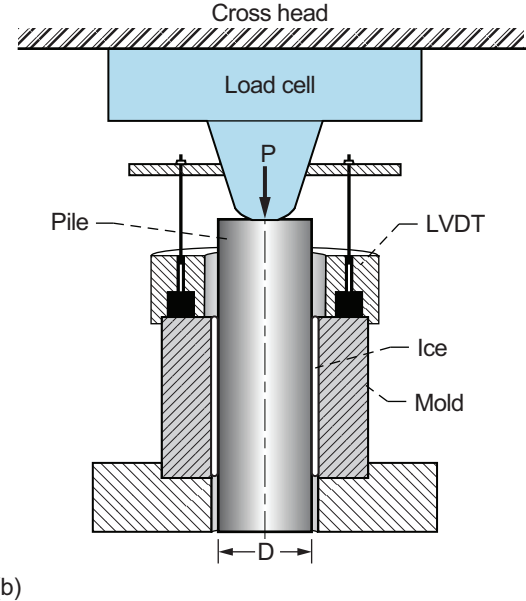
Cross head
Load cell
P
Pile
LVDT
Ice
Mold
D
(b)

Figure 18

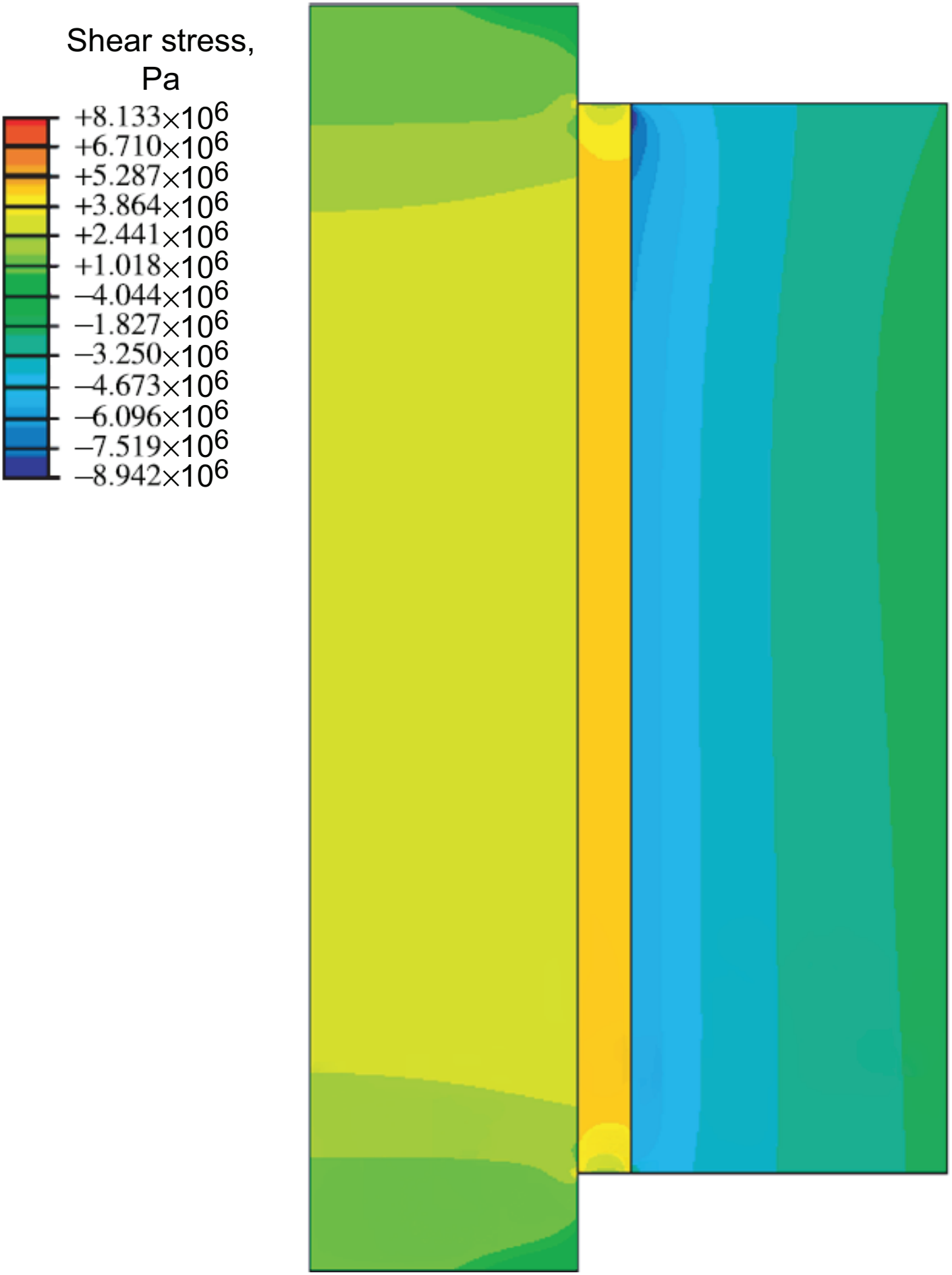
Shear stress, Pa
+8.133×10^6
+6.710×10^6
+5.287×10^6
+3.864×10^6
+2.441×10^6
+1.018×10^6
–4.044×10^6
–1.827×10^6
–3.250×10^6
–4.673×10^6
–6.096×10^6
–7.519×10^6
–8.942×10^6

Figure 19

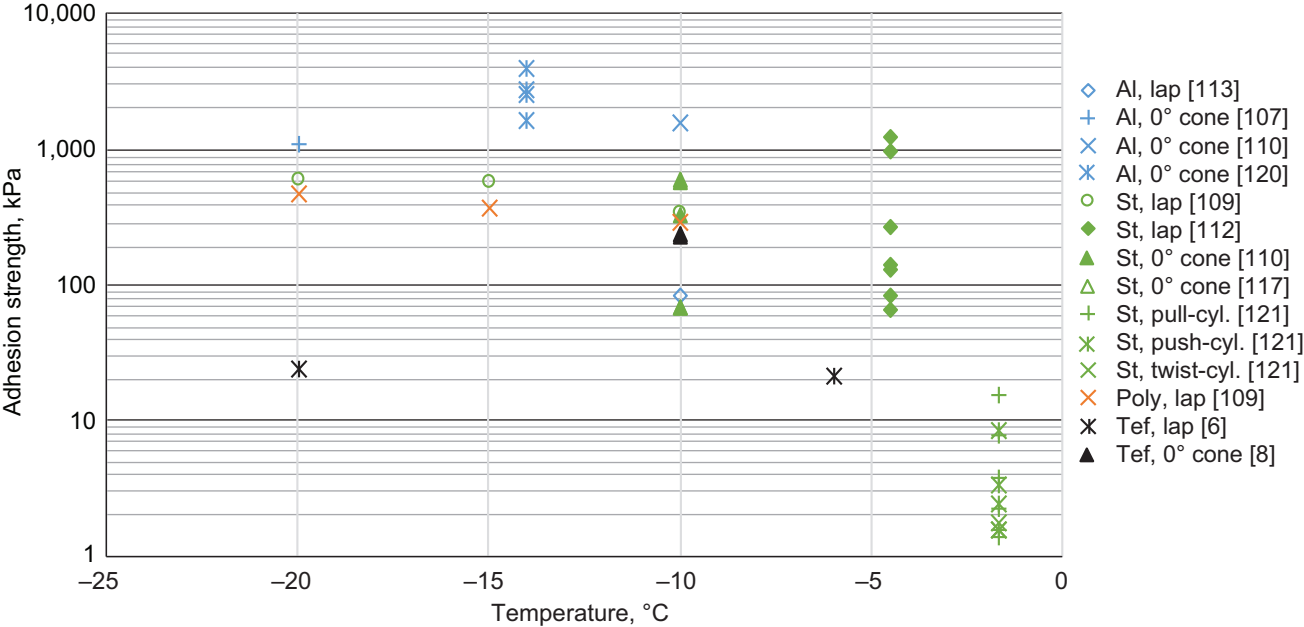
10,000
1,000
100
10
1
Adhesion strength, kPa
–25
–20
–15
–10
–5
0
Temperature, °C
Al, lap [113]
Al, 0° cone [107]
Al, 0° cone [110]
Al, 0° cone [120]
St, lap [109]
St, lap [112]
St, 0° cone [110]
St, 0° cone [117]
St, pull-cyl. [121]
St, push-cyl. [121]
St, twist-cyl. [121]
Poly, lap [109]
Tef, lap [6]
Tef, 0° cone [8]

Figure 20

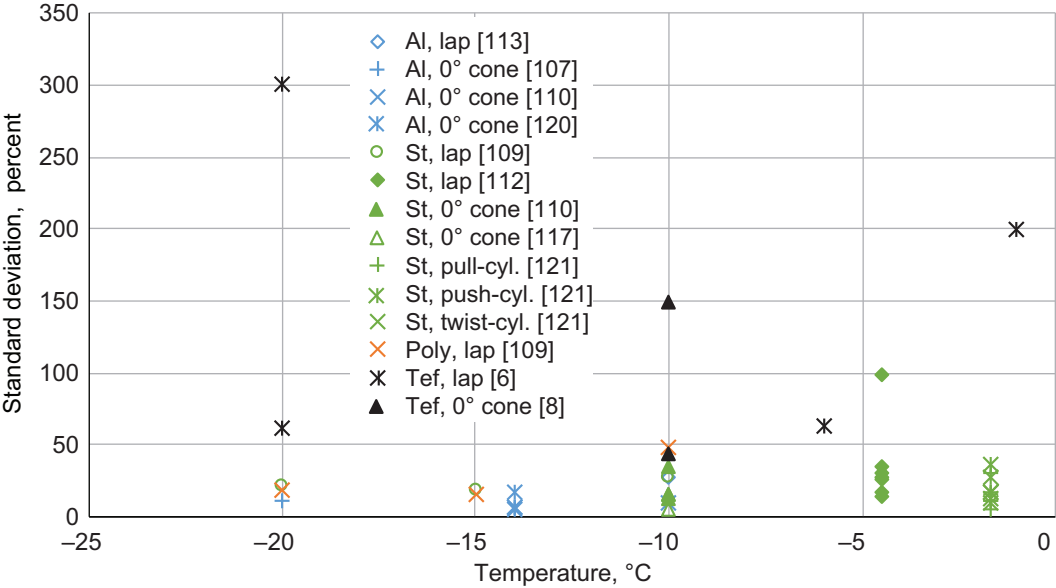
Standard deviation, percent
350
300
250
200
150
100
50
0
–25
–20
–15
–10
–5
0
Temperature, °C
Al, lap [113]
Al, 0° cone [107]
Al, 0° cone [110]
Al, 0° cone [120]
St, lap [109]
St, lap [112]
St, 0° cone [110]
St, 0° cone [117]
St, pull-cyl. [121]
St, push-cyl. [121]
St, twist-cyl. [121]
Poly, lap [109]
Tef, lap [6]
Tef, 0° cone [8]

Figure 21

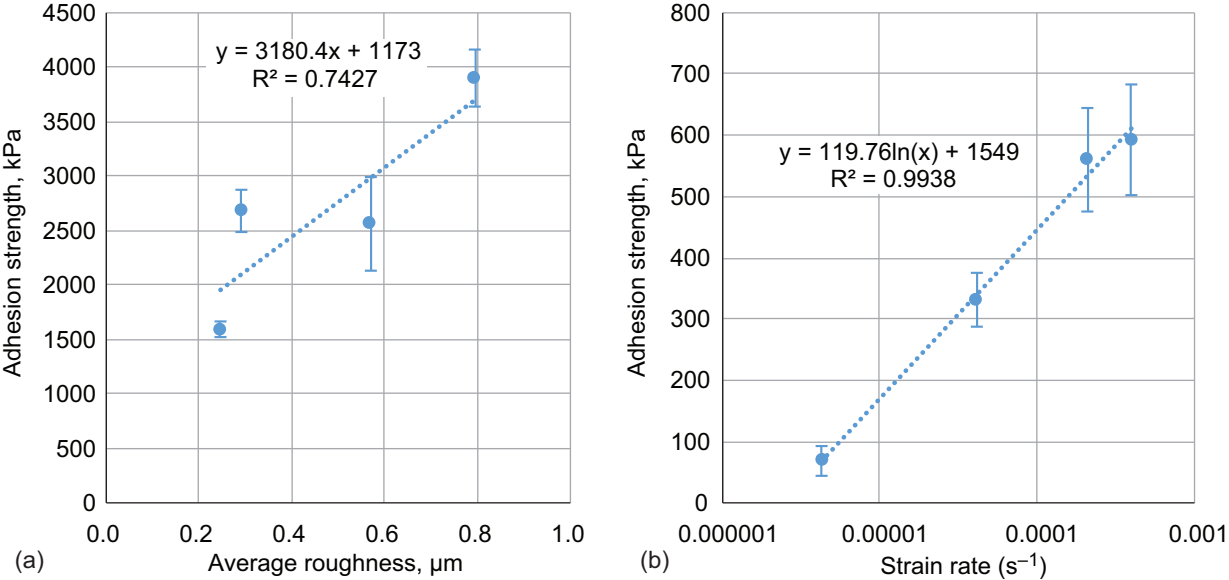
y = 3180.4x + 1173
R² = 0.7427
Adhesion strength, kPa
4500
4000
3500
3000
2500
2000
1500
1000
500
0
0.0
0.2
0.4
0.6
0.8
1.0
(a)
Average roughness, μm
y = 119.76ln(x) + 1549
R² = 0.9938
Adhesion strength, kPa
800
700
600
500
400
300
200
100
0
0.000001
0.00001
0.0001
0.001
(b)
Strain rate (s−1)

Figure 22

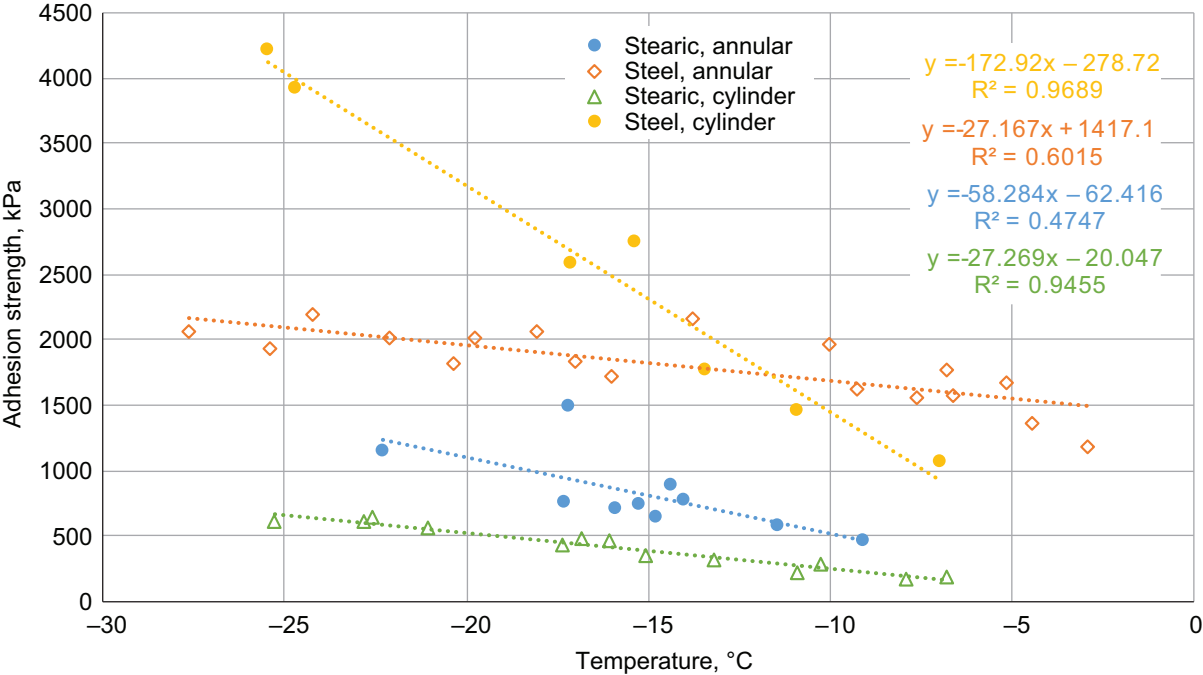
Stearic, annular
Steel, annular
Stearic, cylinder
Steel, cylinder
y =-172.92x – 278.72
R² = 0.9689
y =-27.167x + 1417.1
R² = 0.6015
y =-58.284x – 62.416
R² = 0.4747
y =-27.269x – 20.047
R² = 0.9455
Adhesion strength, kPa
Temperature, °C
4500
4000
3500
3000
2500
2000
1500
1000
500
0
–30
–25
–20
–15
–10
–5
0

Figure 23

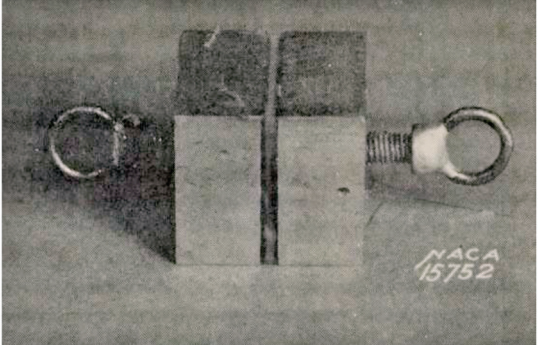

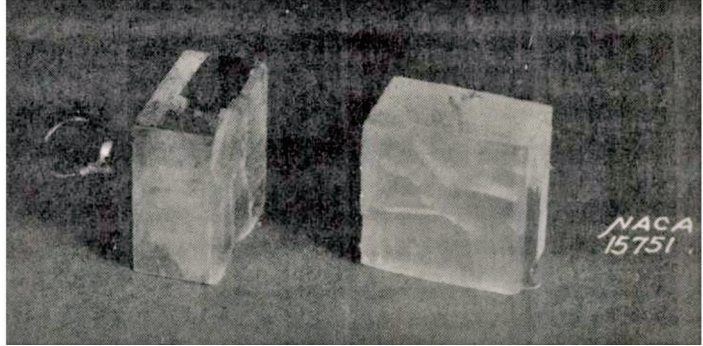

Figure 24

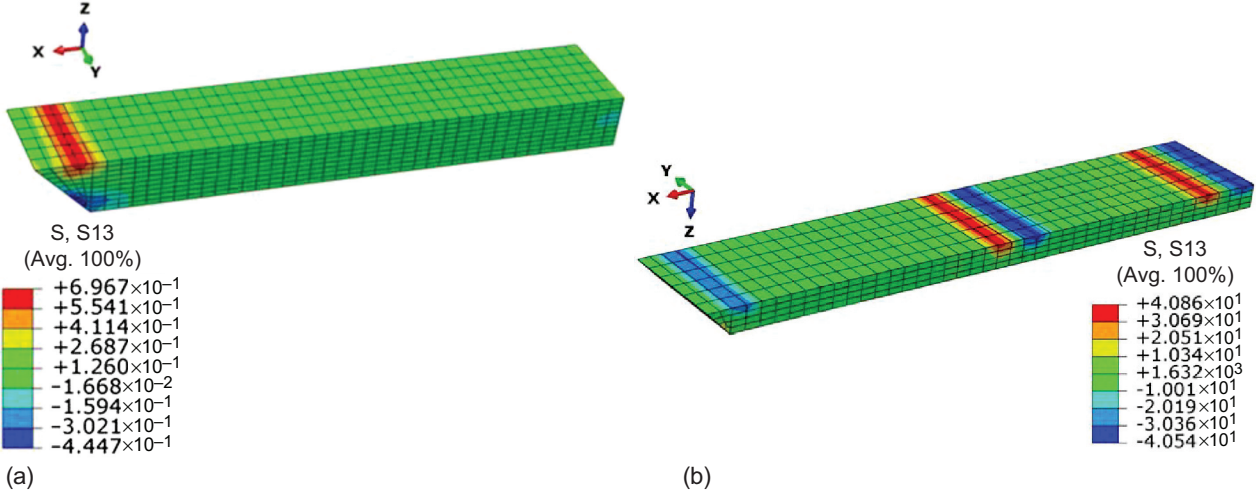
Z
X
Y
S, S13
(Avg. 100%)
+6.967×10−1
+5.541×10−1
+4.114×10−1
+2.687×10−1
+1.260×10−1
−1.668×10−2
−1.594×10−1
−3.021×10−1
−4.447×10−1
(a)
Y
X
Z
S, S13
(Avg. 100%)
+4.086×101
+3.069×101
+2.051×101
+1.034×101
+1.632×103
−1.001×101
−2.019×101
−3.036×101
−4.054×101
(b)

Figure 25

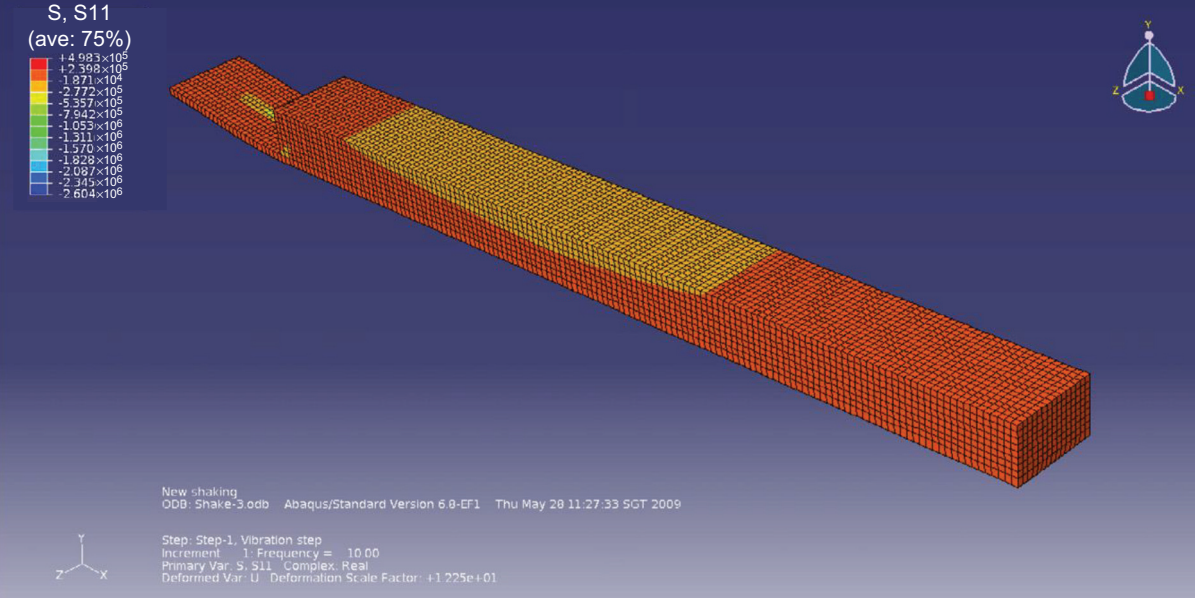
S, S11
(ave: 75%)
+4.983×10^5
+2.398×10^5
-1.871×10^4
-2.772×10^5
-5.357×10^5
-7.942×10^5
-1.053×10^6
-1.311×10^6
-1.570×10^6
-1.828×10^6
-2.087×10^6
-2.345×10^6
-2.604×10^6
New shaking
ODB: Shake-3.odb Abaqus/Standard Version 6.8-EF1 Thu May 28 11:27:33 SGT 2009
Step: Step-1, Vibration step
Increment 1: Frequency = 10.00
Primary Var: S, S11 Complex, Real
Deformed Var: U Deformation Scale Factor: +1.225e+01

Figure 26

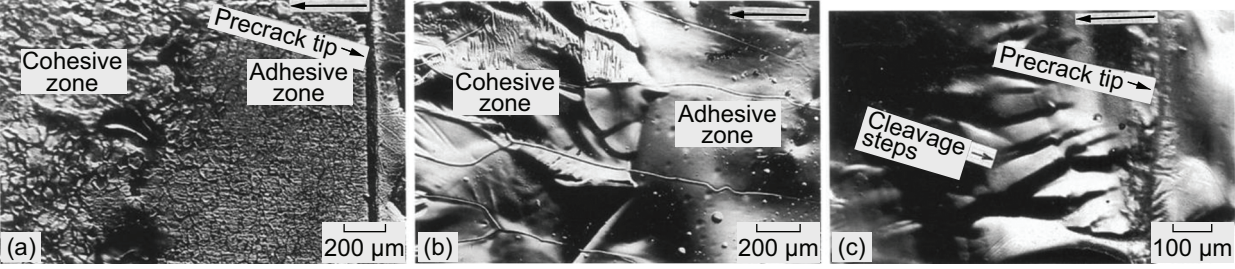
Precrack tip
Cohesive zone
Adhesive zone
(a)
200 μm
Cohesive zone
Adhesive zone
(b)
200 μm
Precrack tip
Cleavage steps
(c)
100 μm

Figure 27

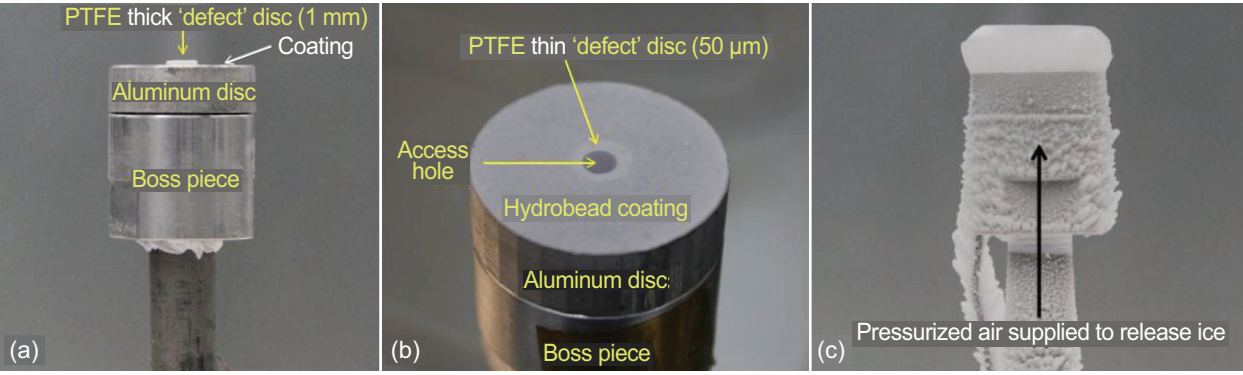
PTFE thick 'defect' disc (1 mm)
Coating
Aluminum disc
Boss piece
(a)
PTFE thin 'defect' disc (50 μm)
Access hole
Hydrobead coating
Aluminum disc
Boss piece
(b)
Pressurized air supplied to release ice
(c)

Figure 28

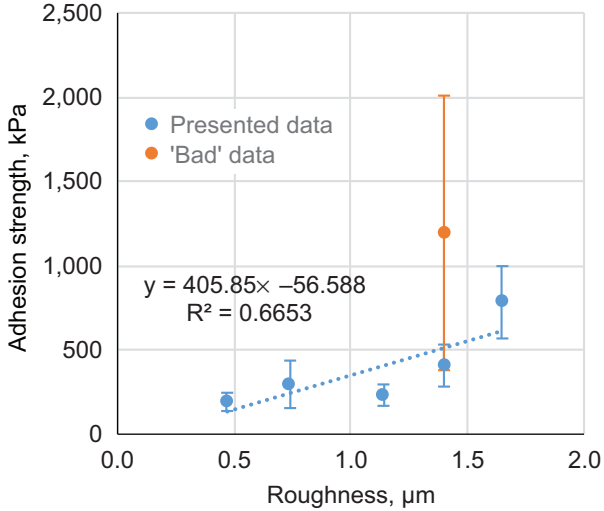

Figure 29

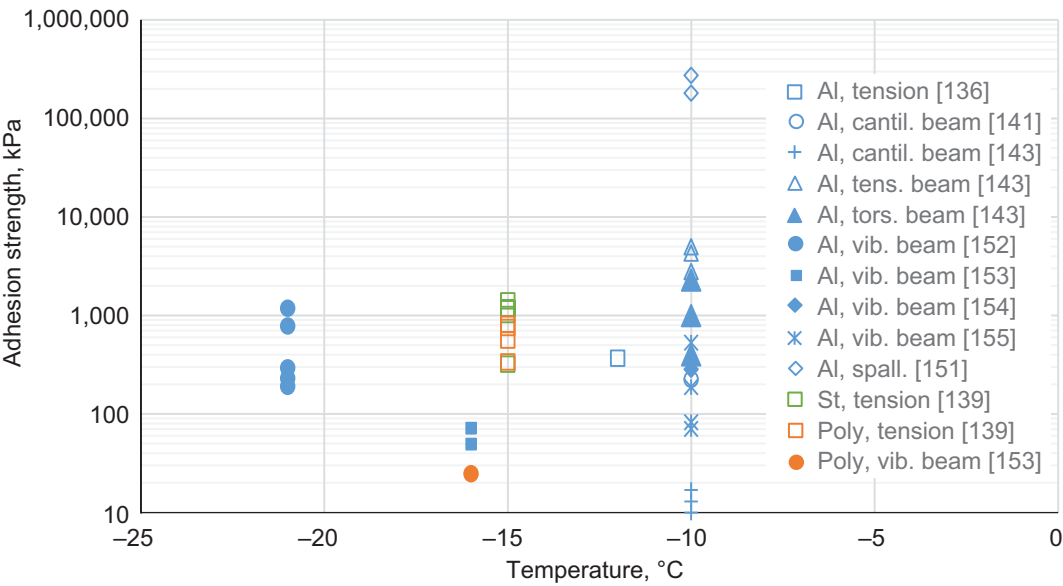

Figure 30


Stardard deviation, percent
200
180
160
140
120
100
80
60
40
20
0
–25
–20
–15
–10
–5
0
Temperature, °C
Al, tension [136]
Al, cantil. beam [141]
Al, cantil. beam [143]
Al, tens. beam [143]
Al, tors. beam [143]
Al, vib. beam [152]
Al, vib. beam [153]
Al, vib. beam [154]
Al, vib. beam [155]
Al, spall. [151]
St, tension [139]
Poly, tension [139]
Poly, vib. beam [153]

Figure 31

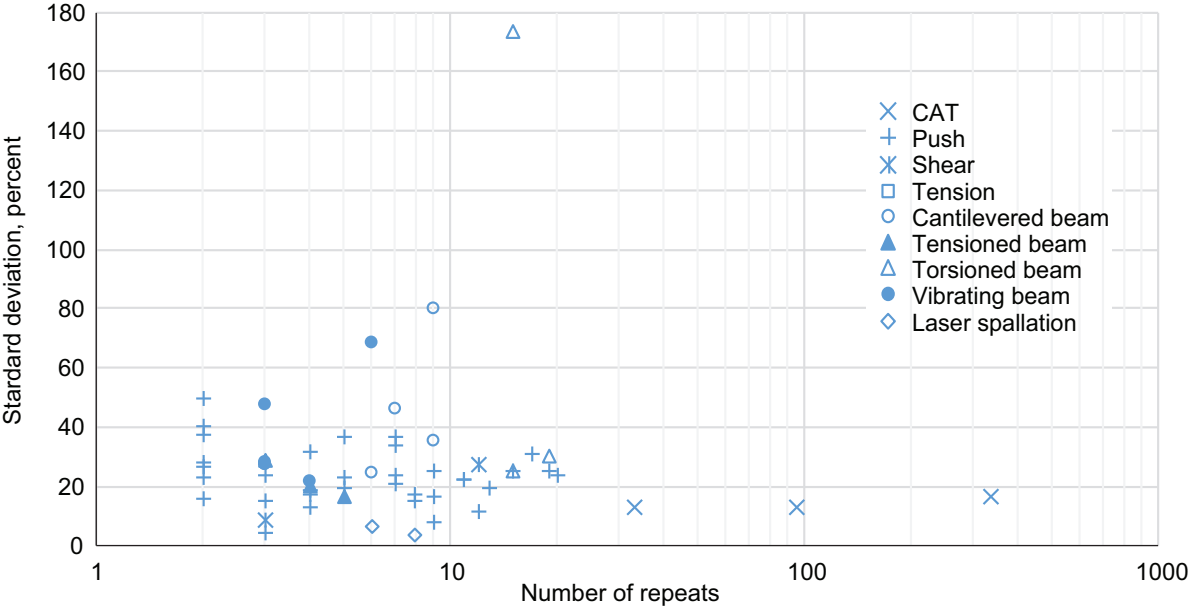

Figure 32

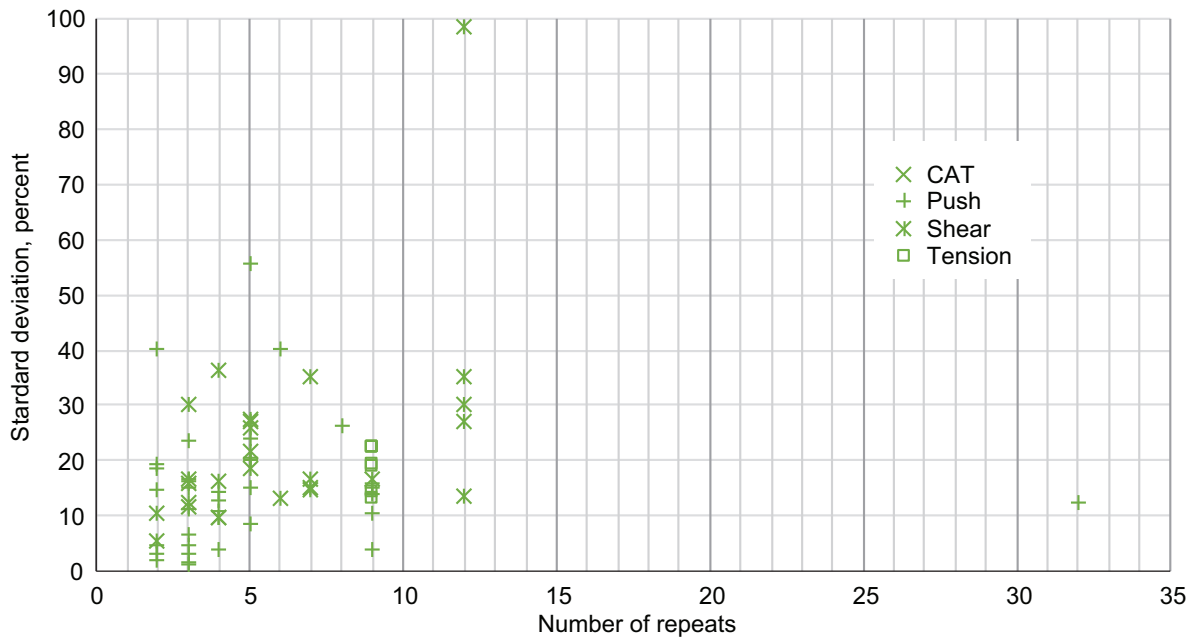

Figure 33

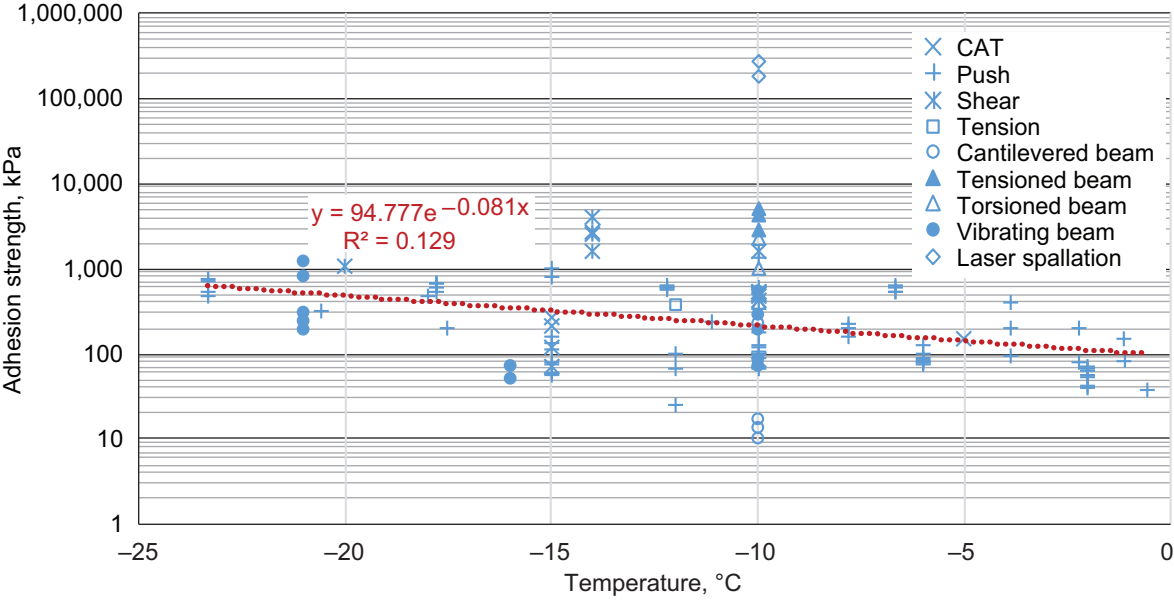

Figure 34

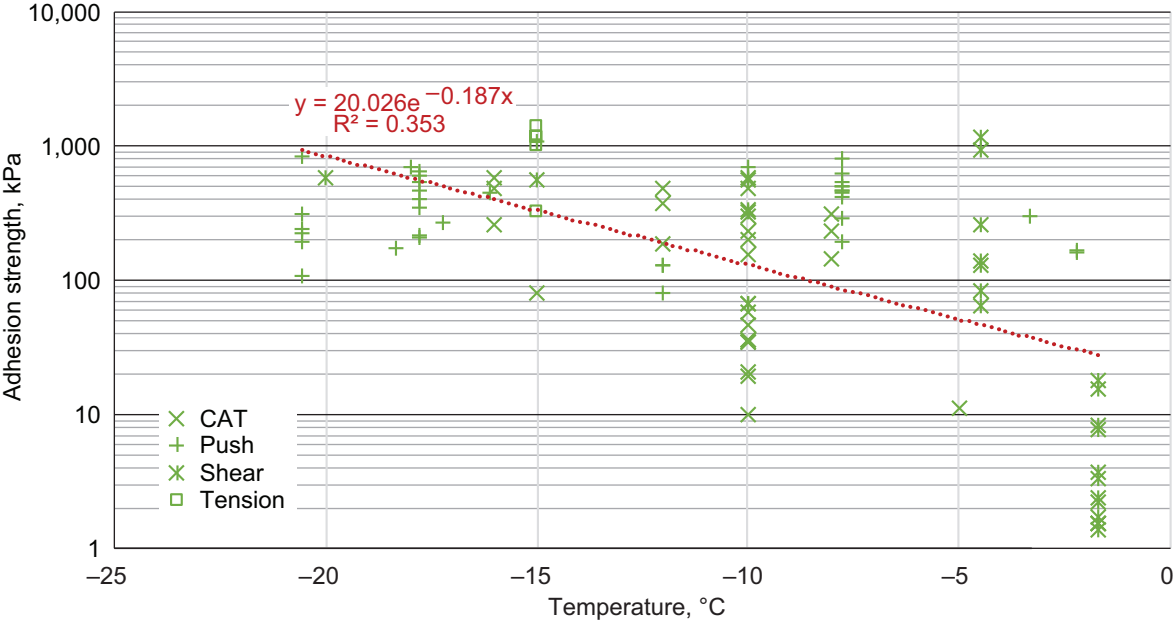

Figure 35

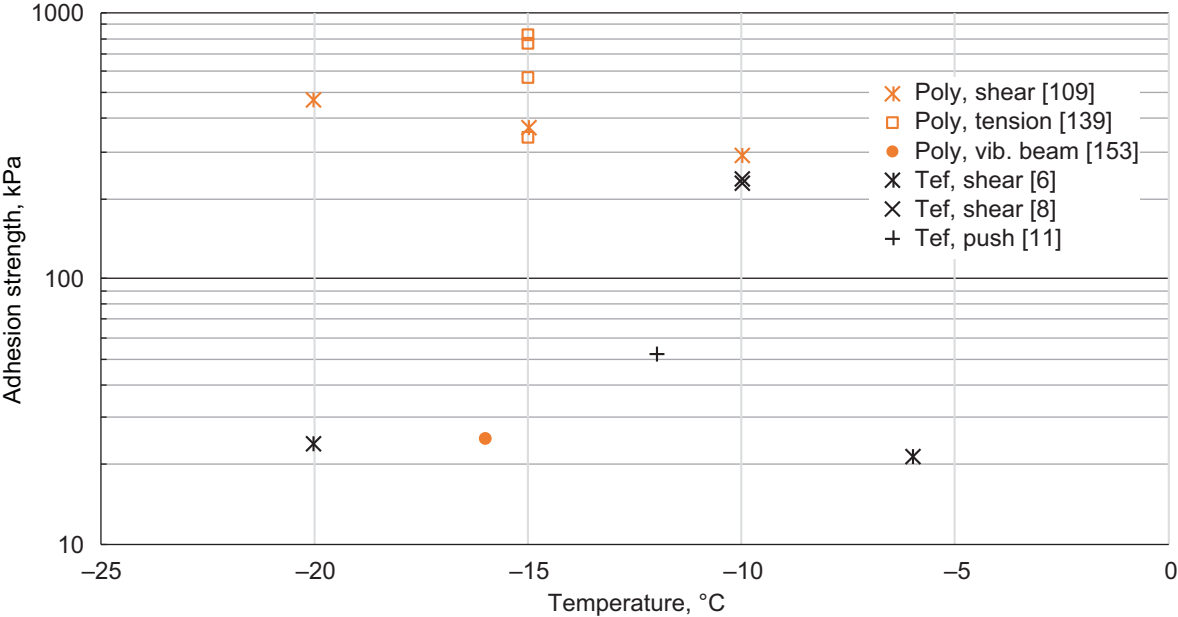
1000
100
10
Adhesion strength, kPa
–25
–20
–15
–10
–5
0
Temperature, °C
Poly, shear [109]
Poly, tension [139]
Poly, vib. beam [153]
Tef, shear [6]
Tef, shear [8]
Tef, push [11]

Figure 36

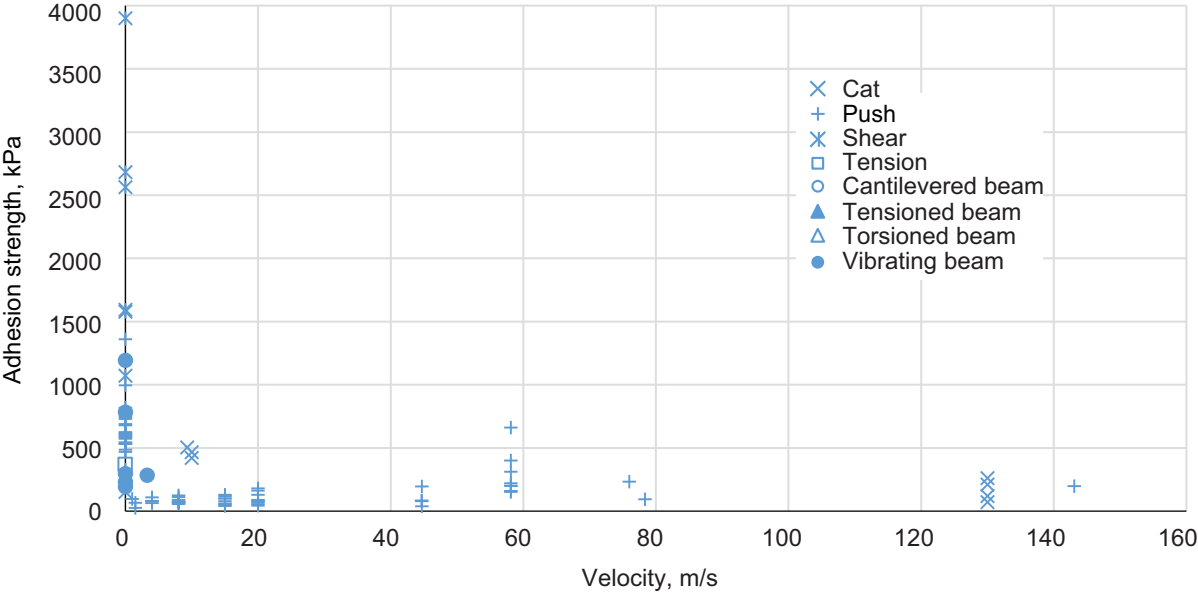
Adhesion strength, kPa
4000
3500
3000
2500
2000
1500
1000
500
0
0
20
40
60
80
100
120
140
160
Velocity, m/s
Cat
Push
Shear
Tension
Cantilevered beam
Tensioned beam
Torsioned beam
Vibrating beam

Figure 37

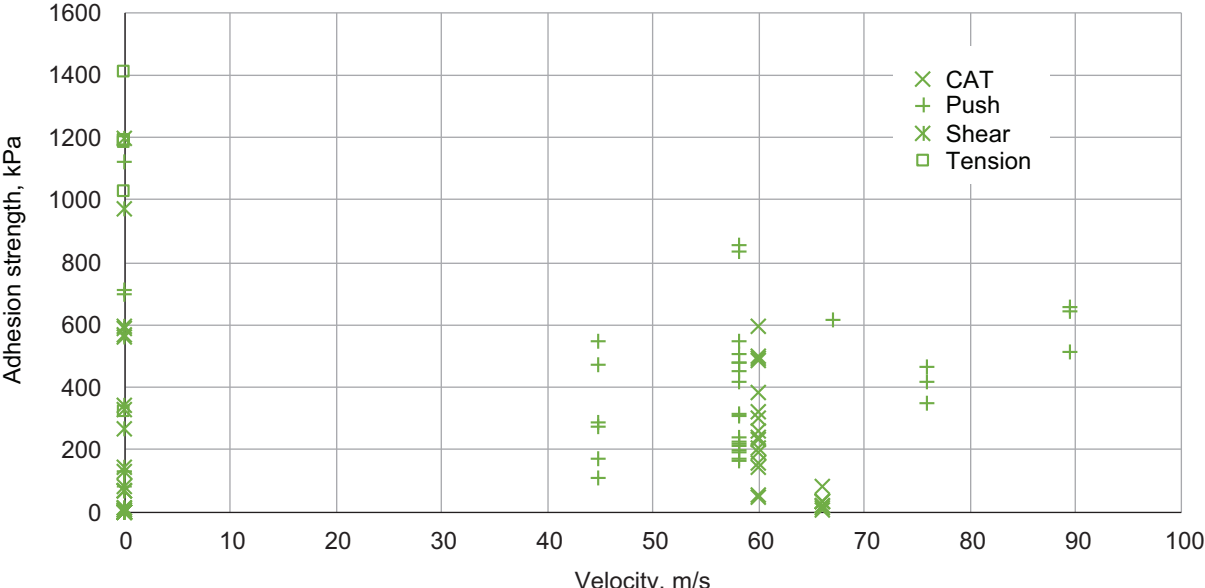
Adhesion strength, kPa
1600
1400
1200
1000
800
600
400
200
0
0
10
20
30
40
50
60
70
80
90
100
Velocity, m/s
CAT
Push
Shear
Tension

Figure 38